#1

THERMODYNAMICS AND KINETICS OF HETEROGENEOUS REACTIONS

J. CLAIR BATTY
ROBERT E. STICKNEY

TECHNICAL REPORT 473

JUNE 2, 1969

MASSACHUSETTS INSTITUTE OF TECHNOLOGY
RESEARCH LABORATORY OF ELECTRONICS
CAMBRIDGE, MASSACHUSETTS 02139

The Research Laboratory of Electronics is an interdepartmental laboratory in which faculty members and graduate students from numerous academic departments conduct research.

The research reported in this document was made possible in part by support extended the Massachusetts Institute of Technology, Research Laboratory of Electronics, by the JOINT SERVICES ELECTRONICS PROGRAMS (U.S. Army, U.S. Navy, and U.S. Air Force) under Contract No. DA 28-043-AMC-02536(E), and by the National Aeronautics and Space Administration (Grant NGR 22-009-091); additional support was received from the M.I.T. Cabot Solar Energy Fund.

Requestors having DOD contracts or grants should apply for copies of technical reports to the Defense Documentation Center, Cameron Station, Alexandria, Virginia 22314; all others should apply to the Clearinghouse for Federal Scientific and Technical Information, Sills Building, 5285 Port Royal Road, Springfield, Virginia 22151.

MASSACHUSETTS INSTITUTE OF TECHNOLOGY

RESEARCH LABORATORY OF ELECTRONICS

Technical Report 473 June 2, 1969

THERMODYNAMICS AND KINETICS OF HETEROGENEOUS REACTIONS

J. Clair Batty and Robert E. Stickney

(Manuscript received January 29, 1969)

Abstract

A generalized treatment of heterogeneous chemical reactions is developed and applied to several sublimation, catalytic, and oxidation processes. The approach is essentially a systematic reformulation of the quasi-equilibrium analyses of Langmuir, Richardson, and others, and it is generalized to apply also to conditions encountered in molecular-beam studies of gas-solid interactions. An advantage of the quasi-equilibrium approach is that it minimizes the use of kinetics to the degree that rate expressions are obtained without assuming detailed kinetic models of the processes.

In Part I, we consider simple sublimation processes (vaporization, thermionic emission, and self-surface ionization) and catalytic reactions (surface ionization and molecular dissociation). The reaction of gaseous oxygen with solid tungsten, molybdenum, and graphite is treated in Part II for steady-state conditions, and this treatment is extended in Part III to the transient case of flash desorption of oxides from a tungsten surface. The theoretical results are compared with existing experimental data, and the agreement is surprisingly good in view of the simplicity of the approach.

TABLE OF CONTENTS

Part I. GENERALIZED TREATMENT OF SIMPLE SUBLIMATION AND CATALYTIC PROCESSES

A. Introduction 1

B. Preliminary Considerations: Gas-Solid Equilibrium 2

C. Model of Sublimation, Thermionic Emission, and Self-Surface Ionization Occurring under Nonequilibrium Conditions 4

D. Model of Catalytic and Gas-Solid Reaction Processes Occurring under Nonequilibrium Conditions 8

1.1 General Description of the Model 8

1.2 Illustrative Applications 11

a. Surface Ionization 11

b. Catalytic Dissociation of Homonuclear Diatomic Gases 12

E. Equilibrium Probability 15

F. Concluding Remarks 19

Part II. EVAPORATION RATES OF VOLATILE SPECIES FORMED IN THE REACTION OF O_2 WITH W, Mo, AND C

A. Introduction 21

B. Summary of a Typical Experiment 22

C. Analysis and Discussion of the O-W Reaction 25

D. Analysis and Discussion of the O-Mo Reaction 33

E. Analysis and Discussion of the O-C Reaction 36

F. Concluding Remarks 38

Part III. FLASH DESORPTION OF OXIDATION PRODUCTS FROM A TUNGSTEN SURFACE

A. Introduction 40

B. Theoretical Analysis 41

C. Comparison of Theoretical and Experimental Results 42

D. Concluding Remarks 47

CONTENTS

Appendix A	Application of Detailed Balancing Considerations to Gas-Solid Interaction Processes	50
Appendix B	Relation of the Quasi-Equilibrium Model to the Statistical Theory of Chemical Reaction Rates	52
Appendix C	Approximate Method for Converting Mass Spectrometric Data to Desorption Rates	56
Appendix D	Estimate of the Desorption Energy of Atomic Oxygen on Tungsten for Varying Coverage	59
References		61

Part I. Generalized Treatment of Simple Sublimation and Catalytic Processes

A. INTRODUCTION

Simple models based on quasi-equilibrium considerations have provided useful approximate descriptions of the rates of a variety of chemical processes occurring at gas-solid interfaces, including sublimation processes, such as the sublimation of neutral atoms[1,2]

$$M(s) \rightleftharpoons M(g), \tag{1}$$

of electrons (thermionic emission)[3,4]

$$e^-(s) + M(s) \rightleftharpoons e^-(g) + M(s), \tag{2}$$

of ions (self-surface ionization)[5,6]

$$M(s) \rightleftharpoons M^+(g) + e^-(g), \tag{3}$$

and catalytic reactions, the most elementary examples being surface ionization[7]

$$A(g) + M(s) \rightleftharpoons A^+(g) + e^-(g) + M(s), \tag{4}$$

the dissociation of homonuclear diatomic gases[8-10]

$$\tfrac{1}{2}A_2(g) + M(s) \rightleftharpoons A(g) + M(s), \tag{5}$$

and the isotope exchange reaction for homonuclear diatomic gases[11]

$$\tfrac{1}{2}A'_2(g) + \tfrac{1}{2}A''_2(g) + M(s) \rightleftharpoons A'A''(g) + M(s). \tag{6}$$

On the other hand, it appears to us that this approach has not yet been fully exploited[12] in connection with gas-solid reactions which result in the formation of volatile products,

$$xM(s) + \frac{y}{2}A_2(g) \rightleftharpoons M_xA_y(g). \tag{7}$$

Our objective is to generalize the existing quasi-equilibrium treatments of processes (1) through (5) so as to obtain a systematic formulation that may be extended to more complex heterogeneous reactions. Specifically, this material serves as the foundation for Parts II and III, in which we consider gas-solid reactions resulting in volatile products [process (7)].

The principal advantage of the quasi-equilibrium approach is the fact that kinetic equations for each step of the reaction are not required except for the rate-limiting step. This advantage is especially important in gas-solid reactions because the steps are often unknown. The philosophy behind the approach is to attempt to formulate approximate descriptions of nonequilibrium processes in terms of simple, quasi-equilibrium models. The procedure is an iterative one, since the simplest model (the one nearest complete equilibrium) is tried first, and then refinements representing nonequilibrium steps are tested to determine if they improve the agreement between "theory" and experiment.

The increasing use of molecular-beam techniques in studies of gas-solid interactions[13,14] has led us to consider the adsorption or sticking probability (called the equilibration probability herein) in some depth. Since molecular beams that are nearly monoenergetic and highly collimated are now being utilized,[15] we begin by defining a differential equilibration probability for molecules of specific speed impinging upon a surface at a specific angle of incidence. A simple model of the equilibration probability is described in Section I-E, and the results are examined with respect to existing experimental data.

B. PRELIMINARY CONSIDERATIONS: GAS-SOLID EQUILIBRIUM

Since the treatment of nonequilibrium processes is based primarily on equilibrium concepts, it is convenient to consider the equilibrium case first. From kinetic theory the rate at which molecules of species i collide with a solid surface of unit area is, for equilibrium conditions,[16]

$$Z_i = p_i(2\pi m_i kT)^{-1/2}, \tag{8}$$

where p_i is the partial pressure of species i, m_i is the molecular mass of i, k is Boltzmann's constant, and T is the temperature of the gas and the solid. A more detailed description of the collision rate is obtained by considering only those molecules having speeds between v and v + dv, and directions within the solid angle $d\omega = \sin\theta\, d\theta d\phi$, where θ and ϕ are defined with respect to the solid lattice in Fig. 1. The differential collision rate for this portion of the impinging molecules is[16]

$$d^3Z_i = \frac{n_i}{\pi^{3/2}}\left(\frac{v}{\alpha_i}\right)^3 \exp\left[-\left(\frac{v}{\alpha_i}\right)^2\right] \sin\theta\cos\theta\, d\theta d\phi dv \tag{9a}$$

$$= \frac{2Z_i}{\pi\alpha_i}\left(\frac{v}{\alpha_i}\right)^3 \exp\left[-\left(\frac{v}{\alpha_i}\right)^2\right] \sin\theta\cos\theta\, d\theta d\phi dv, \tag{9b}$$

where n_i is the number density of i in the gas phase ($n_i = p_i/kT$), and

$$\alpha_i = (2kT/m_i)^{1/2}. \tag{10}$$

From the definitions above it follows that

$$\int_{v=0}^{\infty} \int_{\phi=0}^{2\pi} \int_{\theta=0}^{\pi/2} d^3Z_i = Z_i. \tag{11}$$

The equilibration probability, ζ_i, is defined as the fraction of the collisions that result in adsorption.[18] (For the purposes of this discussion we shall assume that individual particles are distinguishable to the degree that the result of a collision may be

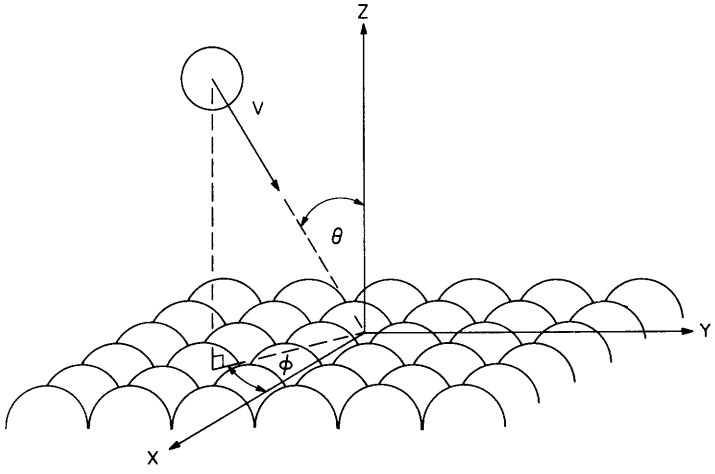

Fig. 1. Geometry of gas-solid interaction. The quantities v, θ, and ϕ refer to a state sufficiently far from the surface that the gas-solid interaction forces are negligible.

classified either as adsorption or as nonadsorption (reflection); however, this assumption is valid only for certain cases, as described in Appendix A.) The differential equilibration probability, $d^3\zeta_i$, is

$$^3\zeta_i = {}^3\Gamma_i / {}^3Z_i, \tag{12}$$

where $^3\Gamma_i$ is the differential adsorption rate (that is, the rate at which molecules of class (v, θ, ϕ) are equilibrated), and we have introduced the superscript 3 as short notation for d^3, such that $^3\zeta_i \equiv d^3\zeta_i$, etc. It is assumed that the definition given in Eq. 12 is based on a sufficiently large number of collisions that $^3\zeta_i$ represents an average over all of the impact points and energy states of the solid that are available to molecules in the class (v, θ, ϕ), as well as an average over all orientations and internal states (vibration and rotation) of the impinging molecules. As a result, $^3\zeta_i$ is a function of v, θ, ϕ, and the thermodynamic properties necessary for specifying the equilibrium thermodynamic state of the system.[18]

Integration of (12) over the possible range of v gives

$$ {}^2\zeta_i = {}^2\Gamma_i / {}^2Z_i = \frac{{}^2\Gamma_i}{Z_i \cos\theta \, d\omega/\pi}, \tag{13} $$

and integration of this over ϕ and θ gives the total equilibration probability for species i,

$$ \zeta_i = \Gamma_i / Z_i. \tag{14} $$

According to detailed balancing arguments given in Appendix A, the differential rate of adsorption, ${}^3\Gamma_i$, must be balanced at equilibrium by an equal but opposite differential rate of desorption of species i from the adsorbate phase, ${}^3R_i$:

$$ {}^3R_i = {}^3\Gamma_i = {}^3\zeta_i \, {}^3Z_i. \tag{15a} $$

Similarly,

$$ {}^2R_i = {}^2\Gamma_i = {}^2\zeta_i \, {}^2Z_i \tag{15b} $$

and

$$ R_i = \Gamma_i = \zeta_i Z_i. \tag{15c} $$

As described in Appendix A, this use of the principle of detailed balance to obtain Eqs. 15 is valid only for those cases in which the equilibrated particles can be distinguished unambiguously from the nonequilibrated particles.

Thermodynamics provides a sufficient set of equations for determining all of the thermodynamic properties of the gas phase if we assume it to behave as a mixture of perfect gases. For example, if there are various chemical reactions, such as those described by Eqs. 1-7, then associated with each independent reaction is an equation based on the equilibrium constant, K_p. These equations, together with $p = \Sigma p_i$, constitute a sufficient set to calculate all of the partial pressures, as will be illustrated in Section I-D. Since rates are outside the domain of thermodynamics, we must turn to kinetic theory to obtain the relation between p_i and Z_i, which is given in (8). The equilibration probability also lies outside thermodynamics, and an accurate theoretical treatment of this property does not exist at present.[19] (A simple model of ζ for diatomic gases will be considered in Section I-E.)

C. MODEL OF SUBLIMATION, THERMIONIC EMISSION, AND SELF-SURFACE IONIZATION OCCURRING UNDER NONEQUILIBRIUM CONDITIONS

By means of a simple model, the equilibrium considerations may be extended to conditions for which the gas and solid phases are not in mutual equilibrium. For simplicity, we shall consider first those gas-solid processes for which the gaseous species

is a component of the solid phase, as in the cases of sublimation, thermionic emission, and self-surface ionization. The results are not original, but they are included for completeness and as illustrations of the scope of the general approach. Since the emphasis is on the approach, many of the details of the derivations are omitted for they may be found in the references cited.

The most frequently used model of sublimation, thermionic emission, and self-surface ionization may be described in terms of a single assumption: The rate of sublimation of atoms, ions, or electrons from a solid remains equal to the equilibrium rate corresponding to the temperature of the solid, regardless of the state of the gas phase. That is, the sublimation rate is assumed to equal the equilibrium rate even in the extreme situation of sublimation into a vacuum, which occurs when the pressures of the volatile species are reduced to essentially zero either by pumping or by applying an electric field in the case of charged particles. We would expect that this assumption is valid only if the sublimation rate is not so high that the thermal and electrical conductivities of the solid are not sufficient to maintain the surface region of the solid in equilibrium with the bulk.

In the case of sublimation of a pure substance, the process is simply

$$M(s) \rightleftharpoons M(g) \tag{1}$$

if the evaporation rates for polymers [$M_2(g)$, $M_3(g)$, etc.] are negligible relative to that for the monatomic species. Under the assumption that the vapor may be treated as a perfect monatomic gas, the equilibrium constant for Eq. 1 is[20]

$$K_p = p_M = \exp\left[-\Delta G^\circ_T/RT \right], \tag{16}$$

where ΔG°_T is the Gibbs free energy of sublimation at temperature T. Since $\Delta G^\circ_T = \Delta H^\circ_T - T\,\Delta S^\circ_T$, (16) may be rewritten

$$p_M = C_M \exp(-\ell_M/kT), \tag{17}$$

where $C_M \equiv \exp(\Delta S^\circ_T/R)$, and ℓ_M is the sublimation enthalpy per atom, $\Delta H^\circ_T/N_o$, where N_o is Avogadro's number. (Since both C_M and ℓ_M are generally weak functions of temperature, they may be assumed to be constants for a limited range of T.) Therefore, the equilibrium sublimation rate, by means of Eqs. 15c, 8, and 17, is

$$R_M = \zeta_M Z_M = \zeta_M p_M (2\pi m_M kT)^{-1/2} \tag{18a}$$

$$= \zeta_M C'_M \exp(-\ell_M/kT), \tag{18b}$$

where $C'_M \equiv C_M(2m_M k)^{-1/2}$ is a weak function of T. According to the model, the sublimation rate of a solid at temperature T will equal this equilibrium rate, regardless

of whether or not the gas phase is in equilibrium with the solid. There is substantial experimental evidence that (18) applies to the sublimation of a variety of solid substances.[1, 2, 21] The equilibration probability, ζ, is commonly called the condensation or evaporation coefficient, and existing experimental data indicate that its value generally is near unity for those metals that sublime predominantly as monatomic species,[1,22] whereas it may be much less than unity for substances subliming as polyatomic species.[22]

The thermionic emission of electrons from a metal may be treated in a similar manner. By analogy with Eq. 16, the equilibrium constant for thermionic emission (Eq. 2) may be written

$$K_p = p_e = \exp\left[\frac{-\left(\mu^\circ_{e(g)} - \mu_{e(s)}\right)}{kT}\right], \tag{19}$$

where ΔG°_T has been replaced by $\left(\mu^\circ_{e(g)} - \mu_{e(s)}\right)$, with $\mu^\circ_{e(g)}$ being the electrochemical potential of the electron vapor at temperature T and unit pressure, and $\mu_{e(s)}$ the electrochemical potential for the electrons in the metal at temperature T. The electrochemical potential of a perfect electron gas, according to quantum statistics,[23] is

$$\mu_{e(g)} \approx kT \ln\left[\frac{1}{2} h^3 p_e (kT)^{-1} (2\pi m_e kT)^{-3/2}\right], \tag{20}$$

where p_e/kT has been substituted for n_e, the electron number density. Recalling that p_e is unit pressure for $\mu^\circ_{e(g)}$, substitution of (20) in (18) yields

$$p_e = 2h^{-3}(2\pi m_e)^{3/2} (kT)^{5/2} \exp(-\phi/kT), \tag{21}$$

where the work function, ϕ, is defined as $-\mu_{e(s)}/N_o$ when the electrostatic field outside the metal is zero. By combining Eqs. 15c, 8, and 21, the equilibrium emission current, J_e, becomes

$$J_e = eR_e = e\zeta_e p_e (2\pi m_e kT)^{-1/2} \tag{22a}$$

$$= \zeta_e A T^2 \exp(-\phi/kT), \tag{22b}$$

where $A = 4\pi e m_e k^2 h^{-3} = 120$ A/cm^2. This expression is the Richardson-Laue-Dushman equation[4] for thermionic emission, and experimental data for clean, uniform metal surfaces indicate that, in agreement with the assumed model, the general form of (22b) is valid under nonequilibrium conditions[4, 24] (for example, when an applied field causes p_e to be less than the equilibrium value).

For some solid substances the rate of sublimation of ions may not be completely

negligible in comparison with the rate of sublimation of neutrals. This is the case of self-surface ionization,[5, 6] and for the purpose of this illustration we shall assume that only the positive ion, $M^+(g)$, is significant. The equilibrium constant for the gas-phase reaction

$$M(g) \rightleftharpoons M^+(g) + e^-(g) \tag{23}$$

may be written

$$K_p = \frac{p_{M^+} p_e}{p_M} = \exp(-\Delta G^\circ_T/RT)$$

$$= \exp\left(-\frac{\Delta H^\circ_T - T\,\Delta S^\circ_T}{RT}\right), \tag{24}$$

where $\Delta G^\circ_T = \Delta H^\circ_T - T\,\Delta S^\circ_T$ is the Gibbs free energy of the reaction described by Eq. 23, with ΔH°_T and ΔS°_T being the corresponding enthalpy and entropy of reaction. Quantum statistics provides expressions for ΔH°_T and ΔS°_T which, when substituted in (24), lead to the following form of the Saha equation[25]:

$$\frac{p_{M^+} p_e}{p_M} = \frac{2g_{M^+}}{g_M}\left[\frac{2\pi k^{5/3}}{h^2}\,\frac{m_{M^+} m_e}{m_M}\right]^{3/2} T^{5/2} \exp(-I/kT), \tag{25}$$

where g denotes the electronic ground-state degeneracy,[26] m is the mass per particle, and the ionization potential, I, is equal to the enthalpy of reaction per atom at 0°K; that is, $I = H^\circ_O/N_o$. Since the gaseous electrons are in equilibrium with the solid, (21) may be substituted for p_e. This step, together with Eqs. 15c and 8 applied to p_{M^+}, after rearrangement, gives the Saha-Langmuir equation for self-surface ionization:

$$\frac{R_{M^+}}{R_M} = \frac{\zeta_{M^+} g_{M^+}}{\zeta_M g_M} \exp\left[-\frac{I - \phi}{kT}\right]. \tag{26}$$

This expression predicts that the ratio of the equilibrium sublimation rates of ions and neutrals depends on their equilibration probabilities, ζ_{M^+} and ζ_M, but is independent of the value of ζ_e. In the derivation of (26) we have assumed implicitly that ϕ is uniform over the surface and that there is a field-free region just outside the solid. Experimental data reported by Scheer and Fine[5] and by Zandberg et al.[6] indicate that the general form of (26) is valid under nonequilibrium conditions of sublimation in vacuum, which is consistent with the assumed model.

As emphasized in the preceding derivation, I is an enthalpy evaluated at 0°K, ϕ is an electrochemical potential at temperature T, and ℓ_M is an enthalpy at temperature T.

Since (a) enthalpy and electrochemical potential are not equivalent properties, and (b) the enthalpies are not evaluated at a common temperature, it is incorrect to write the Schottky relation as[6]

$$\ell_M - \ell_{M^+} = \phi - I, \tag{27}$$

where ℓ_{M^+} is the enthalpy of sublimation of the process $M(s) \rightleftharpoons M^+(s) + e^-(s)$ at temperature T. The correct form of the Schottky relation must involve only enthalpies or electrochemical potentials, all evaluated at the same value of T, or it must restrict (27) to T = 0°K, where enthalpy and electrochemical potential are identical for field-free conditions. Although (27) has been applied incorrectly in some studies,[6] we suspect that the resulting error is generally insignificant in comparison with experimental uncertainties such as surface inhomogeneities.

D. MODEL OF CATALYTIC AND GAS-SOLID REACTION PROCESSES OCCURRING UNDER NONEQUILIBRIUM CONDITIONS

1.1 General Description of the Model

In the preceding discussion of sublimation processes the composition of the gas phase was limited to species that are components of the solid. We now extend the discussion to include (a) catalytic processes in which the gas phase consists of foreign species that are not components of the solid, and (b) gas-solid reaction processes in which the gas phase consists of both foreign species and components of the solid, as well as the reaction products of the two. Following a brief description of the two principal experimental configurations and related terminology, we shall define a model that allows us to extend the equilibrium considerations of Section I-B to catalytic and gas-solid reactions occurring under nonequilibrium conditions.

Investigations of chemical reactions at gas-solid interfaces are often conducted at sufficiently low pressures that the mean-free path is larger than the characteristic dimension of the system. This condition insures that collisions between molecules in the gas phase are negligible in comparison with collisions of molecules with the test surface and chamber walls. Two different configurations are popular for experimental investigations: (i) the isotropic cell,[27] in which the directions (defined by ϕ and θ in Fig. 1) of the molecules impinging upon the test surface are random or isotropic, and their speeds are those of a Maxwellian gas at a temperature, T', that is equal to the temperature of the chamber wall, not the temperature of the test surface, T, and (ii) the molecular beam,[13,14] in which the directions of the impinging molecules are nonisotropic and their speed distribution is either very narrow, as for a nozzle source,[15] or approximately Maxwellian with temperature T', as for a Knudsen source.

In the case of the isotropic cell, the state of the impinging molecules is determined

by T' and Z_i', where Z_i' is the collision rate for species i. (We have chosen to use Z_i' in place of p_i' because it is a more meaningful property under the present conditions. The superscript prime is used here to denote that values of these properties are not necessarily equal to the equilibrium values corresponding to the temperature of the test specimen.) The problem is to compute the desorption rates, R_i', for given experimental conditions defined by the values of T, T', and Z_i'. If we assume, for the present, that the values of the equilibration probabilities are known, then the simple model described below provides a sufficient set of equations to determine R_i'.

The assumptions underlying the model are listed briefly here. A more thorough discussion appears in Section I-F.

1. The impinging molecules may be divided into two classes, one comprising the molecules that are completely equilibrated to the solid, and the other the nonequilibrated molecules.

2. The nonequilibrated molecules are scattered from the surface without undergoing any chemical change.

3. The rate of desorption of each species from the equilibrated adsorbate phase is equal to the rate that would exist if the gas phase were replaced by one that is in equilibrium with the solid, both thermally and chemically, with a pressure sufficient to cause the over-all adsorption rate of each chemical element to be identical to the corresponding rate existing under experimental conditions.

The third assumption may be expressed more clearly if we limit our attention to steady-state conditions. In this case the adsorption and desorption rates may be related in part by conservation equations that are completely independent of the model. For example, if the species impinging upon the surface include A_2, A_2B, and C, while the desorbing species include these plus A, AB, AC, and AM (where M = metal), then the conservation equation for element A is

$$\Sigma_A' = 2\zeta_{A_2}' Z_{A_2}' + 2\zeta_{A_2B}' Z_{A_2B}' = R_A' + 2R_{A_2}' + R_{AB}' + 2R_{A_2B}' + R_{AC}' + R_{AM}', \quad (28)$$

where Σ_A' is the over-all rate of adsorption or desorption of element A. Similar equations may be written for conservation of elements B and C. Now assumption 3 is that the unknown values of R_j' are equal to the equilibrium values R_j that would exist for a gas phase having the same temperature as the solid and having the amounts of the various species adjusted so that the equilibrium composition will provide an over-all adsorption rate of element j, Σ_j, that is equal to Σ_j', the value computed from Eq. 15 for the test (nonequilibrium) conditions. Since this equilibrium composition will generally differ from that of the test conditions, it follows that the adsorption rates for species i, $\zeta_i Z_i$, and $\zeta_i' Z_i'$, are not necessarily equal, even though the over-all rates for the elements, Σ_j and Σ_j', are equal. The physical reasoning behind assumption 3 is that if all species are equilibrated to the solid and to the other adsorbate species in a characteristic time that is negligible with respect to their mean residence time on the surface, then the

adsorbate state (coverage, structure, energy) will depend on the over-all adsorption rates of the elements, Σ_j, and not on the molecular state in which the elements are brought to the surface. It should be emphasized, however, that we are not assuming that ζ_i' is equal to the value for equilibrium conditions.

On the basis of assumption 3 we have reduced the nonequilibrium problem to one of equilibrium, thereby enabling us to employ the thermodynamic treatment outlined in Section I-B. Associated with each independent chemical reaction is an equilibrium constant, K_p, which may be written

$$K_p = \frac{\Pi\left(p_i^{\nu_i}\right)_{\text{products}}}{\Pi\left(p_i^{\nu_i}\right)_{\text{reactants}}} \tag{29a}$$

$$= \frac{\Pi\left[(2\pi m_i kT)^{1/2} Z_i\right]^{\nu_i}_{\text{products}}}{\Pi\left[(2\pi m_i kT)^{1/2} Z_i\right]^{\nu_i}_{\text{reactants}}} \tag{29b}$$

where ν_i represent the stoichiometric coefficients, and Eq. 8 has been used to replace p_i with Z_i. Since equilibrium is assumed, we have $R_i' = R_i = \zeta_i Z_i$, and (29b) may be rewritten

$$K_p = \frac{\Pi\left[(2\pi m_i kT)^{1/2} R_i/\zeta_i\right]^{\nu_i}_{\text{products}}}{\Pi\left[(2\pi m_i kT)^{1/2} R_i/\zeta_i\right]^{\nu_i}_{\text{reactants}}}. \tag{30}$$

Each independent chemical reaction provides an equation similar to (30), and these, together with the conservation equations (28), are sufficient to evaluate the desorption rates, R_i, if it is assumed that the values of K_p, ζ_i', and ζ_i are known. Since values for ζ_i' and ζ_i are not generally available, we are forced either to assume $\zeta_i' = \zeta_i = 1$, or to choose the values that produce the best agreement with experimental data.

The same general approach may be applied to molecular-beam experiments if we account for the fact that the impinging molecules are restricted to a given solid angle (Fig. 1), and their speed distribution may, in the limiting cases, be either Maxwellian or monoenergetic.[15] In the Maxwellian limit the adsorption rate, by analogy with Eq. 13, is

$$^2\Gamma_i' = {}^2\zeta_i' I_i, \tag{31}$$

where I_i is the collision rate (molecular-beam intensity) for species i. Similarly, in

the monoenergetic limit,

$$ {}^{3}\Gamma_i' = {}^{3}\zeta_i' I_i. \tag{32} $$

Since ${}^{2}\zeta_i'$ is not necessarily equal to ${}^{3}\zeta_i'$, even for beams of equal mean molecular energy and intensity, the adsorption rate may depend on the type of molecular beam employed. We shall return to this point in Section I-E.

1.2 Illustrative Applications

a. Surface Ionization

The Saha-Langmuir equation of surface ionization is derived here as an illustrative application of the approach presented in the preceding section. For simplicity, we shall consider a reaction involving only three species: neutral atoms, electrons, and singly charged positive ions. By analogy with the treatment of self-surface ionization, we start by considering the gas-phase reaction

$$ A(g) \rightleftharpoons A^{+}(g) + e(g) \tag{33} $$

for which the equilibrium constant (see Eq. 25) is

$$ K_p = \frac{p_{A^+} p_e}{p_A} = \frac{2g_{A^+}}{g_A} \left[\frac{2\pi k^{5/3}}{h^2} \frac{m_{A^+} m_e}{m_A} \right]^{3/2} T^{5/2} \exp(-I/kT), \tag{34} $$

where I is the ionization potential of A(g), that is, the enthalpy of reaction for Eq. 33 at T = 0°K. Since the gaseous electrons are in equilibrium with the electrons in the solid, p_e is equal to the saturation pressure given by (21). This, together with (15c) and (8), may be substituted in (34) to obtain the following form of the Saha-Langmuir equation, which is analogous to (26):

$$ \frac{R_{A^+}}{R_A} = \frac{\zeta_{A^+} g_{A^+}}{\zeta_A g_A} \exp\left[-\frac{I - \phi}{kT} \right]. \tag{35} $$

According to the model defined in section 1.1, (35) also applies when the gas phase is not in equilibrium with the solid if the over-all adsorption rate for the nonequilibrium case $\left(\Sigma_A' = \zeta_A' Z_A' + \zeta_{A^+}' Z_{A^+}' \right)$ is equal to the over-all desorption rate for the equilibrium case $\left(\Sigma_A = R_A + R_{A^+} \right)$. This condition reduces to

$$ \zeta_A' Z_A' = R_A + R_{A^+} \tag{36} $$

in the special case $Z_A' \gg Z_{A^+}'$. Substitution of (36) in (35), after rearrangement, yields

another common form of the Saha-Langmuir equation:

$$\frac{R_{A^+}}{Z'_A} = \frac{\zeta'_A}{1 + \left(\zeta_A/\zeta_{A^+}\right)\left(g_A/r_{A^+}\right)\exp\left[\frac{I - \phi}{kT}\right]}. \tag{37}$$

Experimental data[7] indicate that the general form of (35) and (37) is valid for a wide variety of gases and solids if the solid surfaces are clean and have uniform properties, and if there is a field-free region just outside the surface.

b. Catalytic Dissociation of Homonuclear Diatomic Gases

There has been a large number of experimental investigations[8-10, 27-30] of catalytic dissociation reactions of the type (Eq. 5),

$$\tfrac{1}{2}A_2(g) + M(s) \rightleftharpoons A(g) + M(s),$$

and the data generally can be explained quite satisfactorily on the basis of a model similar to that described in section 1.1. Since detailed comparisons of the theoretical and experimental results have been reported by Brennan,[10] we shall concentrate on general conclusions that may be obtained on the basis of the quasi-equilibrium approach.

For the special case of equilibrium conditions ($T' = T$) in an isotropic cell, the desorption rate for species A, on the basis of Eqs. 8 and 15c, is

$$R_A = \zeta_A Z_A = \zeta_A p_A (2\pi m_A kT)^{-1/2}. \tag{38}$$

By using the equilibrium constant, $K_p = p_A/p_{A_2}^{1/2}$, Eq. 38 may be rewritten

$$R_A = \zeta_A K_p p_{A_2}^{-1/2} (2\pi m_A kT)^{-1/2}. \tag{39}$$

From (38) and (39) we may conclude that the dependence of R_A on p_A and p_{A_2} will be first-order and half-order, respectively, only if ζ_A is either independent of pressure or a linear function of p_A. Since the dependence of ζ_A on pressure cannot be determined on the basis of thermodynamics, we have the interesting result of R_A, the equilibrium rate of production of atoms by desorption, does not have to have the generally accepted dependence on pressure, $R_A \propto p_{A_2}^{1/2}$, which thermodynamics requires to hold for the equilibrium rate of production of A in the corresponding gas-phase (homogeneous) reaction, $\frac{1}{2}A_2(g) \rightleftharpoons A(g)$.

The preceding result may be explained by recalling that under equilibrium conditions the collision rate, Z_A, is balanced by the desorption rate, R_A, plus the rate of scattering

of nonequilibrated atoms, $(1-\zeta_A)Z_A$:

$$Z_A = R_A + (1-\zeta_A)Z_A. \tag{40}$$

Therefore, the total rate at which species A is returned to the gas phase is equal to Z_A, and this rate does have the expected dependence on $p_{A_2}^{1/2}$:

$$Z_A = p_A(2\pi m_A kT)^{-1/2} = K_p p_{A_2}^{1/2}(2\pi m_A kT)^{-1/2}. \tag{41}$$

Z is a derived thermodynamic property, whereas R and ζ are nonthermodynamic properties because they cannot be measured, or derived from measurable thermodynamic properties, under equilibrium conditions. (This point is considered in Appendix A.) Therefore, we cannot expect to determine the pressure dependence of R_A or ζ_A by thermodynamics alone.

In most experimental investigations of catalytic dissociation the gas temperature, T', is so low that the impinging species is predominantly A_2, whereas the catalyst temperature, T, is sufficiently high to produce a detectable degree of dissociation. Therefore, for an isotropic cell, the conservation equation for A is

$$2\zeta'_{A_2} Z'_{A_2} = 2\zeta'_{A_2} p'_{A_2}\left(2\pi m_{A_2} kT'\right)^{-1/2} = R'_A + 2R'_{A_2} \tag{42}$$

and the model of section 1.1 (Eq. 30) yields

$$K_p = (\pi m_A kT)^{1/4} \frac{\zeta_{A_2}^{1/2}}{\zeta_A} \frac{R_A}{R_{A_2}^{1/2}}. \tag{43}$$

By combining these, we obtain

$$R_A + 2\left[\frac{(\pi m_A kT)^{1/2}}{K_p^2} \frac{\zeta_{A_2}}{\zeta_A^2}\right] R_A^2 = 2\zeta'_{A_2} p'_{A_2}\left(2\pi m_{A_2} kT'\right)^{-1/2}. \tag{44}$$

In the limit $R_A/R_{A_2} \to \infty$, the second term on the left-hand side may be neglected because $K_p \to \infty$, and we obtain

$$(R_A)_{R_A/R_{A_2}\to\infty} = 2\zeta'_{A_2} p'_{A_2}\left(2\pi m_{A_2} kT'\right)^{-1/2}. \tag{45}$$

In this case the rate of desorption of atoms is limited not by thermodynamics but by the adsorption rate (that is, the collision rate and the equilibration probability). Since the

coverage is essentially zero in this limit,[28,30] ζ'_{A_2} will be quite independent of pressure, and we conclude that R_A will exhibit a first-order dependence on p'_{A_2}. In the opposite limit of $R_A/R_{A_2} \to 0$, the first term of (44) may be neglected, and we obtain

$$(R_A)_{R_A/R_{A_2}\to 0} = K_p \left[\frac{\zeta'_{A_2} \zeta_A^2/\zeta_{A_2}}{2m_A k(TT')^{1/2}} \right]^{1/2} \left(p'_{A_2}\right)^{1/2}. \tag{46}$$

Notice that this reduces to (39) as the conditions approach equilibrium. According to (46), under nonequilibrium conditions the pressure dependence of R_A will be half-order only if $\zeta'_{A_2} \zeta_A^2/\zeta_{A_2}$ is either completely independent of p'_{A_2} or varies as $\left(p'_{A_2}\right)^{1/2}$.

Equation (44) may be used, together with existing data on K_p, to calculate the dissociation of various gases for a range of test conditions. Results for H_2, O_2, and N_2 are given in Fig. 2 in terms of the ratio R_A/Σ'_A, which varies from zero at low T and high p'_{A_2} to unity at high T and low p'_{A_2}. The calculations are based on the assumptions that (i) T' = 300°K, (ii) ζ_A, ζ_{A_2}, and ζ'_{A_2} are independent of T and p'_{A_2}, and (iii) no chemical reaction occurs other than dissociation. As shown by Ehrlich[9] and Brennan[10] using similar analyses, the results for H_2 and O_2 agree well with experimental data for reasonable values of the equilibration probabilities. Experimental data for nitrogen are scarce because the dissociation energy of N_2 is so great that the degree of dissociation

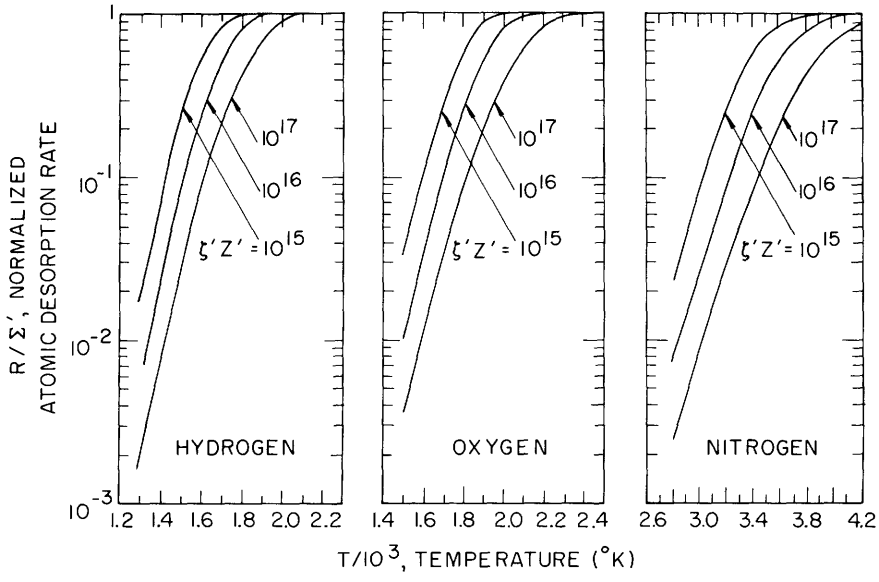

Fig. 2. Theoretical prediction of the degree of dissociation of H_2, O_2, and N_2 by a catalyst at temperature T. Z' is the rate at which molecules impinge upon the surface, ζ' is the equilibration probability, R is the rate at which atoms leave the surface, and Σ' is the maximum possible value of R, i.e., $\Sigma' = 2\zeta'Z'$.

is insignificant, except at extremely high temperatures and low pressures. Some indirect evidence on the dissociation of N_2 by a tungsten catalyst has been reported by Nornes and Donaldson,[31] and their results may be explained quite well by Eq. 46 and Fig. 2. (The qualitative explanation proposed by Nornes and Donaldson[31] is based on the absolute theory of reaction rates which, unlike the quasi-equilibrium approach, requires atomistic models to be assumed for the adsorbate and the reaction mechanism.)

Equation 43 provides a useful relation between R_A and R_{A_2}, as it enables us to determine one of the rates if the other is known. For example, at high temperature and low coverage the kinetic equation for atomic desorption approaches that of a perfect two-dimensional gas[32]

$$R_A = \zeta_A \nu_A [A] \exp(-\chi/kT), \tag{47}$$

where ν_A is the characteristic vibrational frequency of an adsorbed atom, χ is the activation energy for desorption, and [A] denotes the adsorbate coverage (number of atoms adsorbed per unit surface area). According to (43), the corresponding equation for the molecular desorption rate is

$$R_{A_2} = (R_A/K_p)^2 = \zeta_{A_2} \gamma_{A_2} [A]^2 \exp\left[-\frac{2\chi - D}{kT}\right], \tag{48}$$

where

$$\gamma_{A_2} = \zeta_A^2 \nu_A^2 \left\{ \left(\frac{\pi m_A}{h^2}\right)^{3/4} (kT)^{5/4} \left[\frac{g_A^2}{g_{A_2}} \frac{1 - \exp(\Theta_v/T)}{T/2\,\Theta_r} \right]^{1/2} \right\}^{-1} \tag{49}$$

and statistical mechanics has been used to express K_p in the form[33]

$$K_p = \left(\frac{\pi m_A}{h^2}\right)^{3/4} (kT)^{5/4} \left[\frac{g_A^2}{g_{A_2}} \frac{1 - \exp(\Theta_v/T)}{T/2\,\Theta_r} \right]^{1/2} \exp\left[\frac{-D}{2kT}\right], \tag{50}$$

where h is Planck's constant, Θ_r and Θ_v are the rotational and vibrational characteristic temperatures, respectively, g is the ground-state degeneracy, and D is the dissociation energy (the enthalpy of the reaction $A_2 \rightleftharpoons 2A$ at 0°K). This approach has been employed by Ehrlich[9] and McCarroll.[29]

E. EQUILIBRATION PROBABILITY

Since the equilibration probability, ζ, plays an important role in the present analysis and in succeeding applications, it is considered briefly here. The subject has been

reviewed recently,[19] so we shall concentrate on one particular model which appears to provide a useful approximate explanation of some cases of dissociative adsorption.

If the gaseous species impinging upon a surface is atomic rather than molecular, then ζ depends entirely on the probability of the atom losing sufficient energy to the solid that it becomes "trapped" by the gas-solid potential. Although energy transfer may also influence the equilibration probability of molecules, the rate-limiting process may instead be the dissociation of molecules into adsorbed atoms. For example, ζ may depend either on the probability of the impinging molecules having sufficient energy to pass over an activation-energy barrier,[34,35] or on the probability of adsorbed molecules migrating to preferred sites for dissociation before desorption occurs.[36,9,35] Only the former process will be considered here, and we shall use the model of Lennard-Jones[34] in a manner suggested recently by van Willigen.[37]

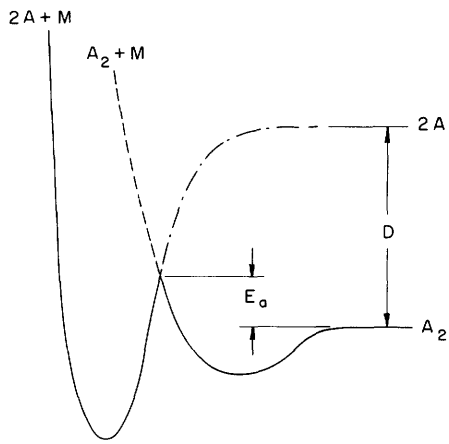

Fig. 3.

Schematic representation of the gas-solid interaction potentials for the case of activated dissociative adsorption of molecules, A_2, on the surface of solid M. E_a is the activation energy separating the molecular (A_2+M) and atomic (2A+M) adsorption states, and D is the dissociation energy for $A_2(g) \rightarrow 2A(g)$.

As illustrated in Fig. 3, the gas-solid interaction potential may be of such a nature that the atomic and molecular states of adsorption are separated by an activation-energy barrier of height E_a. For simplicity, we shall assume that E_a is constant over the entire surface.[38] Molecules impinging with speed v at angles θ and ϕ (Fig. 1) will be able to adsorb dissociatively $\left[\frac{1}{2} A_2(g) \rightleftharpoons A(ad)\right]$ only if their energy is large enough to carry them over barrier E_a. That is, the differential equilibration probability of molecules in class (v,θ,ϕ) is[39]

$$ {}^3\zeta = \begin{cases} 0 & \text{if } \frac{1}{2} m(v \cos\theta)^2 < E_a \\ \zeta_o & \text{if } \frac{1}{2} m(v \cos\theta)^2 \geq E_a \end{cases} \qquad (51) $$

where ζ_o is a transmission coefficient representing the fact that some molecules with sufficient energy will not pass over E_a because of quantum-mechanical reflection or of steric considerations.[35] We shall simplify the following discussion by assuming that ζ_o is independent of v, θ, and ϕ. If the gas phase is in equilibrium with the solid, then

from Eq. 13 we obtain

$$ {}^2\zeta = \frac{{}^2\Gamma}{{}^2Z} = \frac{1}{{}^2Z} \int_0^\infty {}^3\zeta \, {}^3Z \, dv \tag{52a} $$

which, with the aid of (96) and (51), may be expressed as

$$ {}^2\zeta = \int_{v^*}^\infty 2\zeta_o (v/a)^3 \exp[-(v/a)^2] \, dv/a \tag{52b} $$

$$ = \zeta_o \left[1 + \frac{E_a}{kT} \sec^2 \theta \right] \exp\left(- \frac{E_a}{kT} \sec^2 \theta \right), \tag{52c} $$

where the lower limit of integration is $v^* = (2E_a/m)^{1/2} \sec \theta$. Therefore the ratio of ${}^2\zeta$ for angle of incidence θ to that for normal incidence ($\theta = 0$) is

$$ \frac{{}^2\zeta(\theta)}{{}^2\zeta(0)} = \frac{E_a + kT \cos^2 \theta}{(E_a + kT) \cos^2 \theta} \exp\left(- \frac{E_a}{kT} \tan^2 \theta \right) \tag{53} $$

and, with the aid of Eq. 13, the corresponding ratio of the differential adsorption rates is

$$ \frac{{}^2\Gamma(\theta)}{{}^2\Gamma(0)} = \frac{{}^2\zeta(\theta)}{{}^2\zeta(0)} \cos \theta = \frac{E_a + kT \cos^2 \theta}{(E_a + kT) \cos \theta} \exp\left(- \frac{E_a}{kT} \tan^2 \theta \right). \tag{54} $$

Since ${}^2R(\theta) = {}^2\Gamma(\theta)$ according to detailed balancing (see Eq. 15b), it follows that (54) also provides an expression for ${}^2R(\theta)/{}^2R(0)$.

Equation 54 is identical to that used by van Willigen[37] to explain his experimental observation that the angular distribution of hydrogen desorbing from various metals is not simply proportional to cos θ. Van Willigen's data are rather convincing evidence for the existence of the activation-energy barrier, and similar results have been obtained independently by Saltsburg and Smith.[40]

Integration of Eq. 52c over θ and ϕ yields

$$ \zeta = \zeta_o \exp(-E_a/kT). \tag{55} $$

Expressions of this form are commonly assumed for the "sticking probability" of gas molecules on solid surfaces.[9, 10, 30, 35]

The preceding equations must be modified if the gas phase is not in equilibrium with the solid. In the case of a monoenergetic molecular beam, ${}^3\zeta'$ is given by (51) with ζ_o replaced with ζ_o' to denote that this transmission coefficient may depend on the temperature of the solid.[39] The dependence of ${}^3\zeta'$ on θ is illustrated in Fig. 4 for

$\frac{1}{2} mv^2 = \sqrt{2}\, E_a$, and the results suggest that experimental measurements of this sort could be used to determine E_a and/or to test the validity of the model.

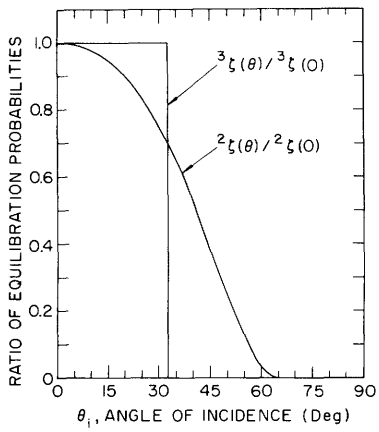

Fig. 4. Illustration of the theoretical dependence of the equilibration probability, ζ, on angle of incidence, θ_i. The curve for $^3\zeta(\theta)/^3\zeta(0)$ was computed from Eq. 51 for the case of a monoenergetic molecular beam of energy $\frac{1}{2} mv^2 = \sqrt{2}\, E_a$. The curve for $^2\zeta(\theta)/^2\zeta(0)$ was computed from Eq. 56 for a Maxwellian beam of temperature $T' = \sqrt{2}\, E_a/2k$.

For a molecular beam having a Maxwellian speed distribution with temperature T', we obtain by analogy with (52c),

$$^2\zeta' = \zeta'_o \left[1 + \frac{E_a}{kT'} \sec^2\theta\right] \exp\left[-\frac{E_a}{kT'} \sec^2\theta\right]. \tag{56}$$

As illustrated in Fig. 4 for $T' = \sqrt{2}\, E_a/2k$, Eq. 56 predicts that $^2\zeta'$ – and therefore the adsorption rate – decreases markedly with increasing angle of incidence, θ. This trend has been observed recently by Saltsburg and Smith[40] in a molecular-beam study of the H_2-D_2 exchange reaction on a nickel catalyst. Equation 56 also predicts that $^2\zeta'$ increases markedly with T', and this characteristic has been observed by Krakowski and Olander[30] for the dissociation of an H_2 beam by a heated tantalum catalyst. They report that their data indicate that $E_a \approx 1.4$ kcal/gmole if it is assumed that the equilibration probability is simply proportional to $\exp(-E_a/kT')$. (According to the present model it would have been more appropriate to use Eq. 56.) It is interesting to note that Krakowski and Olander's assumption that H_2 desorbs with a random or cosine distribution is inconsistent with the fact that $E_a \neq 0$. In their case, however, E_a is so small that, on the basis of the present model, the deviation from a cosine distribution would not be very significant. By combining the model described in section 1.1 with that described here, it follows that T', the temperature of the gas, controls the adsorption rate through Eq. 56, whereas T, the temperature of the solid, controls the desorption rate and angular distribution through Eq. 54.

For the case of an isotropic cell in which the gas is at temperature $T' \neq T$, the equilibration probability is obtained by integrating (56) over θ and ϕ. The result is identical to (55), except that T' appears in place of T.

The present model of the equilibration probability is extremely primitive, but it

does appear to provide a partial explanation of existing data. Since there is experimental evidence that ζ is a function of the adsorbate coverage,[35] the results given here are valid at best only for constant coverage or in the limit of zero coverage. Also, the assumption that E_a is constant over the entire surface is of questionable validity, especially in the case of polycrystalline surfaces.

F. CONCLUDING REMARKS

We have attempted to present a systematic and generalized reformulation of the quasi-equilibrium approach that has been used in various forms in the past to derive approximate expressions for the rates of sublimation and catalytic processes. The scheme of systematization was to consider each process as a chemical reaction that may be described in terms of an equilibrium constant. Generalization was strived for by stating the assumptions and selecting the variables in such a manner that the approach would not be limited to a single class of reactions, materials, or experimental conditions.

The present approach does not constitute an exact or rigorous theory of heterogeneous reactions because the quasi-equilibrium model is a drastic approximation.[41] There is substantial evidence, however, that it provides useful descriptions of the simple sublimation and catalytic processes considered herein, and in Parts II and III we illustrate its success in providing a semiquantitative description of the production of volatile products in the reaction of gaseous oxygen with solid surfaces. The approach no doubt will fail to explain the experimental data for certain reactions or systems, but in such cases it will provide a standard for comparison which may help to identify the rate-limiting step responsible for deviation from quasi-equilibrium.

The assumptions underlying the present treatment of catalytic reactions warrant further discussion because they have not previously been considered in detail. The validity of the first assumption rests upon the possibility of dividing the impinging molecules into two classes, one comprising the molecules that are equilibrated to the solid before returning to the gas phase, and the other the nonequilibrated molecules. Some support for this assumption may be obtained from Smith and Fite's experimental data[27] on the catalytic dissociation of an H_2 molecular beam by a tungsten surface heated to ~2500°K. Their results show that, although the H atoms desorbing from the surface have the diffuse spatial distribution generally expected in the case of complete equilibration, the spatial distribution of the H_2 molecules is lobular or nondiffuse, thereby indicating incomplete momentum accommodation of a significant fraction of the impinging molecules. McKinley's experimental data[27] on the catalytic dissociation of Cl_2 by a heated tungsten surface also indicate that a fraction of the impinging molecules are scattered without achieving complete energy accommodation with the solid.

Although our experimental data are evidence that not all of the molecules impinging upon a catalytic surface will attain complete energy and momentum accommodation, they

do not prove the second assumption that dissociation occurs only for those molecules that are thermally equilibrated (complete energy and momentum accommodation). The fact that Smith and Fite[27] observed a diffuse spatial distribution for the H atoms desorbing from the surface is an indirect indication that the majority of the atoms were accommodated, but a more direct proof would be desirable (for example, measurements of the velocity distribution of the desorbed H atoms). Another indirect indication of the validity of the second assumption, as well as of the other two assumptions, is the agreement of predictions based on these (or equivalent) assumptions with experimental data.[7-10, 29-31]

The third assumption essentially constitutes a definition of the term equilibration, the statement being that the equilibrated species desorb at a rate equal, by detailed balancing, to the adsorption rate that would exist if the gas phase were replaced by an equilibrium mixture having the same over-all adsorption rate for each chemical element. An alternative statement of this assumption is that the state of the adsorbate phase at a given temperature depends only on the rates at which the various chemical elements are added to the phase, and not on the molecular composition of these elements before adsorption, except for the effect of the molecular form of the impinging species on ζ, the equilibration (adsorption) probability. We would expect this assumption to be a reasonable approximation unless (i) the reaction mechanism of the catalytic process requires that certain molecular species be supplied directly from the gas phase, as in the case of the Rideal-Eley mechanism,[42] or (ii) the relaxation rates associated with both the energy distribution and the chemical composition of the adsorbate phase are not sufficiently large relative to the desorption rates to maintain equilibrium conditions when the composition of the impinging gas deviates from equilibrium. Results presented in Part II indicate that this assumption may be valid even in complex gas-solid reactions such as the oxidation of tungsten.

We have given considerable attention to the equilibration probability ζ because it is a principal parameter in the present treatment. Unfortunately, there is a deficiency of experimental and theoretical information on the equilibration process for temperatures much above 300°K. As a result, ζ is essentially a defined parameter in the present treatment and it constitutes the only adjustable parameter that may be altered to maximize the agreement of the theoretical results with experimental data. If agreement can be obtained with "reasonable" values of ζ, then we have indirect support for the quasi-equilibrium approach. A more convincing test of the approach would be to compare the resulting values of ζ with values measured by an independent means.

It has been suggested to us recently by J. C. Keck that the quasi-equilibrium treatment presented here for heterogeneous processes may also be formulated in a manner analogous to the statistical theory of reaction rates for homogeneous (gas-phase) processes. This formulation, which is considered briefly in Appendix B, has the advantage of illustrating that both heterogeneous and homogeous reactions may be treated by a generalized statistical theory.

Part II. Evaporation Rates of Volatile Species Formed in the Reaction of O_2 with W, Mo, and C

A. INTRODUCTION

At normal temperatures and pressures the chemical reaction of a gas with a solid generally results in the formation of condensed products, such as a solid oxide, nitride, hydride, or halide, rather than volatile (gaseous) products.[47,48] At high temperatures and low pressures, however, the formation of volatile products is favored over the growth of the condensed phase for some gas-solid systems. Recently, the formation of volatile products in gas-solid reactions has received increased attention (see Table 1)

Table 1. Summary of mass spectrometric investigations of gas-solid chemical reactions resulting in volatile products.

System	Experimental Technique			Investigators
	Isotropic Source* (steady-state)	Modulated Molecular Beam (transient)	Flash Desorption (transient)	
O-W	X			Schissel and Trulson[59]
O-W	X			Berkowitz-Mattuck et al.[60]
O-W		X		Steele[61]
O-W			X	Ptushinskii and Chuikov[62]
O-W			X	McCarroll[63]
O-Mo	X			Steele[64]
O-Mo	X			Berkowitz-Mattuck et al.[60]
O-Ge	X			Lever[65]
I-W			X	McCarroll[66]
Cl-Ni		X		Smith and Fite[67]
Cl-Ni	X			McKinley[68]
Cl-Y	X			McKinley[69]
Br-Ni	X			McKinley[70]
Br-W			X	McCarroll[71]
F-Ni	X			McKinley[72]

*In an isotropic source the molecules impinging upon the test specimen have random (isotropic) directions.

because the process is encountered in a wide variety of technological areas, including thermionic energy conversion,[49] ion propulsion,[50] high-temperature gas dynamics,[51] metal purification[52] and depositions,[53] and incandescent[54] and arc lamps.[55]

The principal objective of the present work is to derive approximate expressions for the evaporation rates of volatile products formed in steady-state gas-solid reactions at sufficiently low pressures that gas-phase processes may be neglected in comparison with the processes occurring at the gas-solid interface. The analysis is based upon the quasi-equilibrium approach described in Part I, and results have been obtained for the reaction of oxygen with tungsten, molybdenum, and carbon. We have chosen these three systems because (i) the thermodynamic property data necessary for computing the equilibrium constants K_p are available, (ii) experimental data exist for comparison in the case of O-W and O-Mo, and (iii) the adsorption and desorption of oxygen on W and on Mo have been investigated recently in our laboratory.[56-58]

As described in Part I, our approach is to use equilibrium thermodynamics to the greatest possible degree, since this simplifies the analysis by minimizing the need for assuming detailed kinetic models of the individual steps of the reaction. Kinetic theory is used only to obtain an expression for the rate at which molecules impinge upon the solid surface; this expression is essentially a boundary condition between the gas and solid phases, and it enables us to determine rates in terms of thermodynamic properties. Comparison of the theoretical results with existing experimental data for O-W, O-Mo, and O-C leads to the conclusion that the rate-limiting step, for all three systems, is the "trapping" or temporary adsorption of the impinging oxygen molecules for a sufficient time during which they become equilibrated both to the solid and to the other adsorbed species. This nonthermodynamic effect is accounted for by introducing an equilibration probability (for example, a sticking probability) into the present treatment, and we demonstrate that with this one adjustable parameter it is possible to obtain close agreement with experimental data for O-W and for O-Mo.

B. SUMMARY OF A TYPICAL EXPERIMENT

A brief summary of a typical mass-spectrometric experiment of gas-solid chemical reactions is given here because it simplifies and clarifies the description of the analysis presented in the succeeding section. Schissel and Trulson's study[58] of O-W has been selected for this illustration because a detailed comparison of our theoretical results with their experimental data will be made in Section II-C. Similar mass spectrometer apparatus have been used by others in investigations of a variety of gas-solid systems (see Table 1).

The principal features of Schissel and Trulson's apparatus are shown in Fig. 5. Valve A is used to adjust p'_{O_2}, the O_2 pressure in the chamber, to the desired steady-state value. Since p'_{O_2} is restricted to sufficiently low values that the mean-free path

for gas-phase collisions exceeds the characteristic dimension of the chamber, free-molecule flow conditions are insured and the O_2 molecules impinging upon the tungsten surface are at the temperature of the water-cooled chamber walls (~300 °K). On the basis of kinetic theory,[72] the rate at which O_2 molecules impinge upon the unit area of the surface is

$$Z'_{O_2} = p'_{O_2} \Big/ \left(2\pi m_{O_2} kT'\right)^{1/2}, \tag{57}$$

where m_{O_2} is the molecular mass, k is Boltzmann's constant, T' is the gas temperature (300°K), and the superscript prime denotes, as in Part I, that the gas properties are not the equilibrium values corresponding to the temperature of the tungsten specimen, T, which may be varied independently of the gas temperature by adjusting the

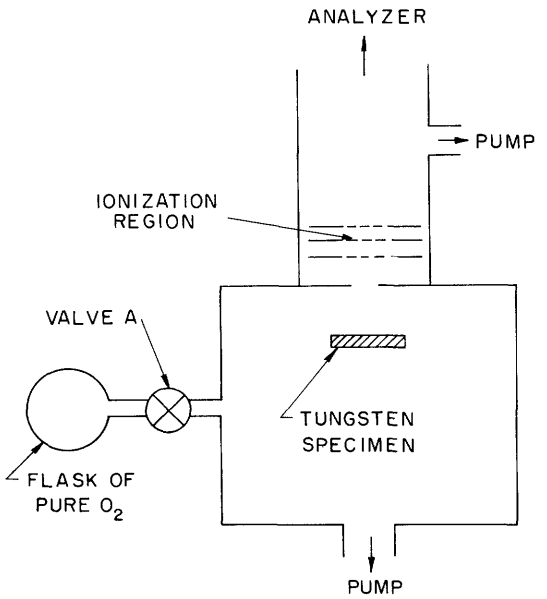

Fig. 5. Typical experimental apparatus used in mass-spectrometric studies of gas-solid chemical reactions.

heating current passing through the specimen. A portion of the impinging molecules react with the solid atoms to form various products which, at the temperatures and pressures considered here, are so volatile that they evaporate at a rate that prevents the growth of a solid oxide phase on the tungsten surface. Since (a) the evaporating oxide species will condense readily upon the chamber wall, (b) the evaporating atomic oxygen will recombine on the wall to form molecules, and (c) gas-phase collisions are insignificant, it seems reasonable to assume that a negligible fraction of the evaporating species is scattered back to the tungsten surface, with the result that the dominant species impinging upon the specimen is molecular oxygen with a rate given by Eq. 57.

As illustrated in Fig. 5, the apparatus is so designed that a fraction of the reaction products evaporating from the specimen will pass directly through the ionization region

of the mass spectrometer before undergoing collisions with walls, electrodes, or other molecules. The mass-spectrometer output signal for species i is an ion current, I_i^+, which may be used to compute the evaporation rate R_i' in the manner described by

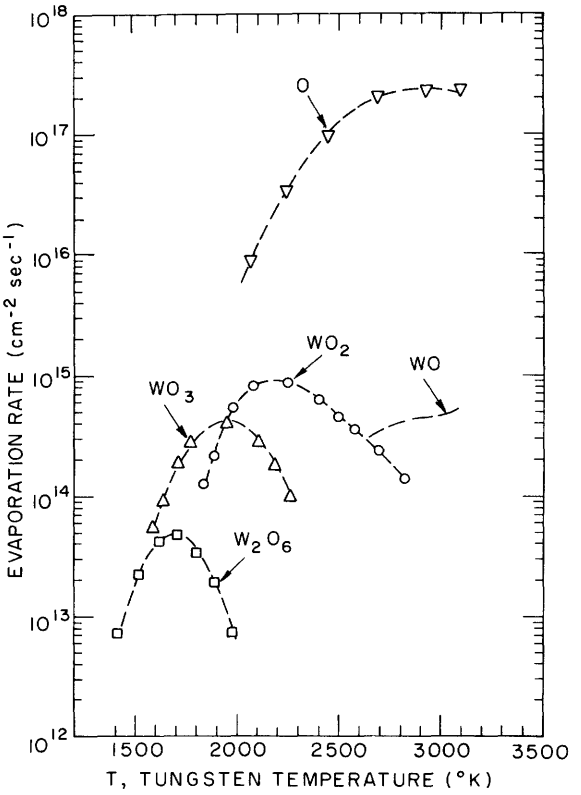

Fig. 6.
Experimental data on the evaporation rates of volatile species formed in the chemical reaction of gaseous O_2 with solid tungsten (Schissel and Trulson[13]). The O_2 pressure and temperature are held constant at 2.1×10^{-4} Torr and 300°K, corresponding to an impingement rate of $Z'_{O_2} = 7.5 \times 10^{16}$ molecules cm^{-2} sec^{-1}.

Schissel and Trulson.[59] (Their calculation is based implicitly on the assumption that the angular distribution of the evaporating products is the same (for example, a cosine distribution) for all species; however, as mentioned in Part I, there is evidence that this assumption may not be valid for all gas-solid systems.) The experimental data for R_i' vs T at a chamber pressure of $p'_{O_2} = 2.1 \times 10^{-4}$ Torr are shown in Fig. 6. Each data point corresponds to a mass spectrometer measurement made under steady-state conditions at various values of T', the temperature of the tungsten specimen, but all for the same conditions of the impinging O_2 molecules; that is, $p'_{O_2} = 2.1 \times 10^{-4}$ Torr, T' = 300°K, so from Eq. 57, $Z'_{O_2} = 7.5 \times 10^{16}$ cm^{-2} sec^{-1}. The results show that the formation of the simplest species, O and WO, is favored as T increases, and at the highest temperature $R'_O \approx 2\, Z'_{O_2}$ because the tungsten surface acts as an efficient catalyst for dissociating the impinging O_2 molecules. Data for the evaporation (desorption) rate of O_2 do not appear in Fig. 6 because the signal corresponding to this species was obscured by the O_2 pressure maintained in the chamber.

C. ANALYSIS AND DISCUSSION OF THE O-W REACTION

If the model described in Part I is applied to the O-W reaction with conditions identical to those in Schissel and Trulson's experiment, then the basic assumptions may be restated in more specific terms.

1. The impinging O_2 molecules may be divided into two classes: the first comprising the molecules that are trapped or temporarily adsorbed by the surface for the sufficient time that they are equilibrated, both thermally and chemically, to the tungsten and to the other adsorbed species; the second, the nonequilibrated molecules. If ζ'_{O_2} represents the probability that an impinging molecule will be equilibrated, then the rate of adsorption (equilibration) is

$$\Gamma'_{O_2} = \zeta'_{O_2} Z'_{O_2}, \tag{58}$$

where Z'_{O_2} is defined by (57).

2. The nonequilibrated molecules are scattered from the surface without undergoing chemical change; that is, they rebound as O_2 molecules. (The speed and angular distributions of the scattered nonequilibrated molecules are of no consequence in the present analysis because these properties were not determined by Schissel and Trulson.)

3. The rate of evaporation of each species from the equilibrated adsorbate phase is equal to R_i, the rate that would exist if the O_2 gas were replaced by a gas mixture that is in thermal and chemical equilibrium with the tungsten specimen and has a total pressure sufficient to cause Σ_O, the over-all adsorption rate of oxygen atoms, to equal $2\zeta'_{O_2} Z'_{O_2}$, the corresponding rate for the actual (nonequilibrium) conditions.[73] This condition, together with the steady-state expression for conservation of oxygen, may be written

$$\Sigma_O = 2\zeta'_{O_2} Z'_{O_2} = R_O + 2R_{O_2} + R_{WO} + 2R_{WO_2} + 3R_{WO_3} + 6R_{W_2O_6} + 8R_{W_3O_8} + 9R_{W_3O_9} + 12R_{W_4O_{12}}. \tag{59}$$

We have not included oxides above W_4O_{12} because this represents the upper limit of existing thermodynamic data, and species above W_3O_9 were not detected by Schissel and Trulson. The nine evaporation rates appearing in (59) may be related through the equilibrium constants of their respective reactions, which may be represented by a generalized stoichiometric expression

$$xW(s) + \frac{y}{2} O_2(g) \rightleftharpoons W_xO_y(g). \tag{60}$$

The corresponding expression for the equilibrium constant is

$$K_p = p_{W_xO_y} \Big/ \left(p_{O_2}\right)^{y/2}. \tag{61}$$

Since the equilibrium constants are expressed in terms of p_i, the equilibrium partial pressures, a relation between p_i and R_i is needed in order to obtain as many equations as unknowns. This relation is simply that, according to the principle of detailed balance, the equilibrium evaporation rate of species i is equal to the equilibrium adsorption (equilibration) rate

$$R_i = \zeta_i Z_i = \zeta_i p_i / (2\pi m_i kT)^{1/2}, \tag{62}$$

where ζ_i is the equilibration probability for species i under equilibrium conditions. Since the values of ζ_i are unknown, we are forced to assume that $\zeta_i = 1$ for all of the product species. With this assumption, (62) may be used to rewrite (61) as

$$K_{W_xO_y} = (2\pi kT)^{1/2(1-y/2)} \left(\frac{M_{W_xO_y}}{M_{O_2}^{y/2}} \right)^{1/2} \frac{R_{W_xO_y}}{R_{O_2}^{y/2}}, \tag{63}$$

where M represents the molecular weight and $K_{W_xO_y}$ may be computed from[74]

$$K_{W_xO_y} = \exp\left[- \left(\Delta H^o_{W_xO_y} - T\Delta S^o_{W_xO_y} \right) \Big/ RT \right], \tag{64}$$

where $\Delta H^o_{W_xO_y}$ and $\Delta S^o_{W_xO_y}$ are the enthalpy and entropy of formation listed in the JANAF Table.[76] Equations 59, 63, and 64 are a sufficient set for computing the evaporation rates, R_i, for given values of T, Z'_{O_2}, and ζ'_{O_2}. With the aid of a digital computer, we have obtained results for a variety of conditions.

The results presented in Fig. 7 were computed for comparison with Schissel and Trulson's data shown in Fig. 6 for $Z'_{O_2} = 7.5 \times 10^{16}$ cm^{-2} sec^{-1}. In this first comparison we have assumed that $\zeta'_{O_2} = 1$ throughout the entire range of temperature. Notice that although the general features of the computed curves are qualitatively similar to the corresponding features of the experimental data, the quantitative agreement becomes increasingly poor with decreasing T. One possible explanation of this discrepancy is that ζ'_{O_2} decreases as T decreases, which is a reasonable relationship because the adsorbate coverage increases with decreasing T, and it is known that the "sticking probability," which is almost identical to ζ, decreases with increasing coverage for a wide variety of gas-solid systems.[77] This suggested explanation is also supported by the fact that, by applying the conservation relation described by Eq. 59 to the experimental data, we find that ζ'_{O_2} must have the temperature dependence shown in Fig. 8 if the adsorption rate of O atoms is to equal the over-all evaporation rate of O,

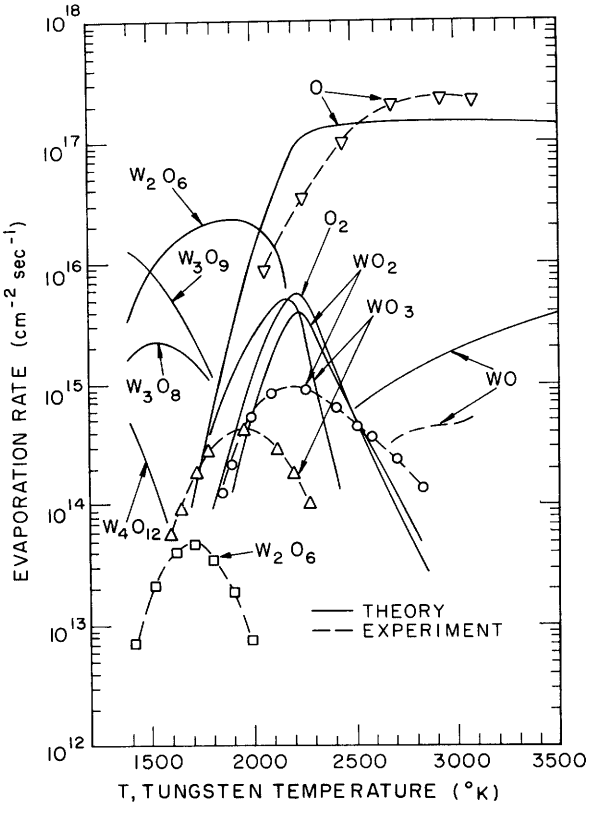

Fig. 7

Comparison of theoretical evaporation rates with corresponding experimental data of Schissel and Trulson[58] for the chemical reaction of gaseous O_2 with solid tungsten. The experimental data are identical to those shown in Fig. 6; therefore, $Z'_{O_2} = 7.5 \times 10^{16}$ cm^{-2} sec^{-1}. The theoretical results are based on tabulated thermodynamic data[76] and on the simplifying assumption that $\zeta'_{O_2} = 1$ over the entire range of conditions.

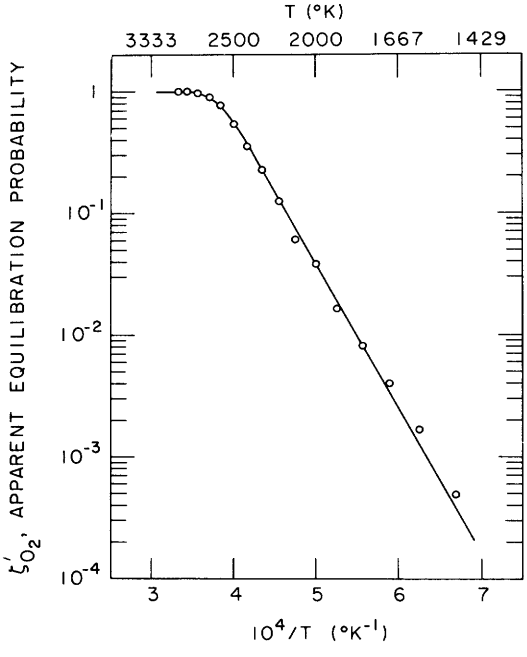

Fig. 8

Apparent equilibration probability, ζ'_{O_2}, as a function of T, the temperature of the tungsten specimen. (Calculated from Schissel and Trulson's experimental data.)

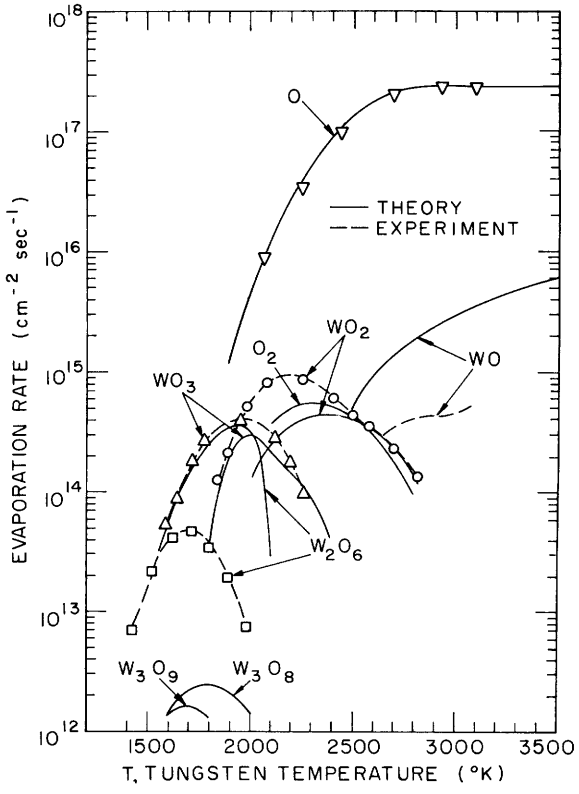

Fig. 9.

Comparison of theoretical evaporation rates with corresponding experimental data for the reaction of O_2 with W. The conditions and assumptions are identical to those for Fig. 7, except that the computations are based on the equilibration probability shown in Fig. 8, rather than on the assumption that $\zeta'_{O_2} = 1$, and Z'_{O_2} is assumed[78] to be 1.19×10^{17} molecules cm^{-2} sec^{-1}.

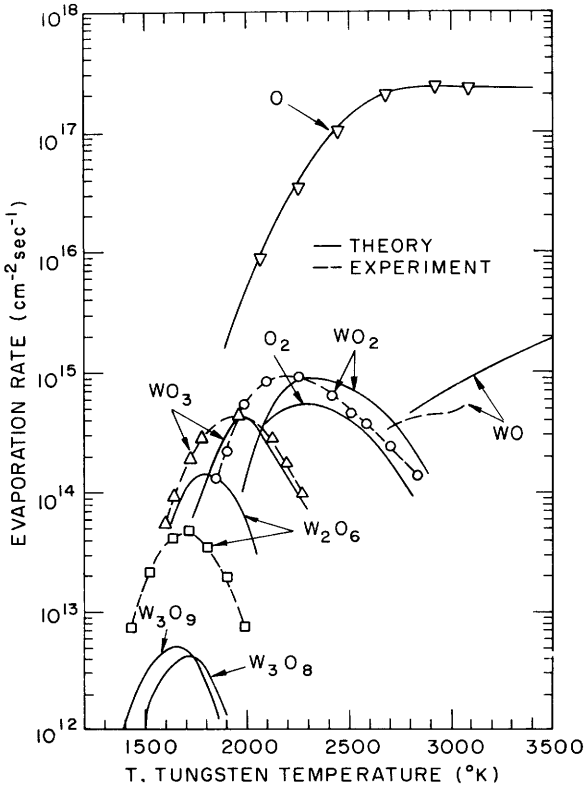

Fig. 10.

Comparison of theoretical evaporation rates with corresponding experimental data for the reaction of O_2 with W. All conditions and assumptions are identical to those for Fig. 9, except that the enthalpy of formation data have been adjusted within their limits of probable error to obtain better agreement (see Table 2).

that is, the right-hand side of (59). (Figure 8 is based on the assumption[78] that Z'_{O_2} = 1.19×10^{17} cm^{-2} sec^{-1} and ζ'_{O_2} = 1 for T > 2900°K; also, since the evaporation rate of O_2 could not be detected experimentally because of the high background pressure of O_2, we have used a theoretical estimate[79] of R_{O_2}.) The data for ζ'_{O_2} vs 1/T could be transformed to the form ζ'_{O_2} vs coverage if we had an expression for the coverage as a function of T and Z'_{O_2}, or of T, p'_{O_2}, and T'; at present, however, this information does not exist for O-W. The results presented in Fig. 9 were computed by using this apparent equilibration probability in place of the initial assumption of ζ'_{O_2} = 1, and we see that the agreement between theory and experiment is much closer than in Fig. 7.

Table 2. Enthalpies of formation for the volatile species formed in the reaction of gaseous O_2 with solid tungsten.

Species	$\Delta H_{f298.15}$ (kcal/gmole)	
	JANAF Value[75]	Value Used in Fig. 10
O(g)	59.559 ± 0.03	59.559
WO(g)	101.6 ± 10	109.6
WO_2(g)	18.3 ± 7	15.0
WO_3(g)	-70.0 ± 7	-70.0
W_2O_6(g)	-278.2 ± 10	-268.2
W_3O_8(g)	-408.7 ± 10	-398.7
W_3O_9(g)	-483.6 ± 10	-473.6
W_4O_{12}(g)	-670.2 ± 10	-660.2

Note: By definition, the enthalpies of formation of O_2(g) and W(s) are zero at 298.15°K and 1 atm.

We suspect that one cause of the discrepancy between theory and experiment in Fig. 9 is the inaccuracy of the thermodynamic property data that is available for the tungsten oxides. Since the equilibrium constant is an exponential function of ΔH^o and ΔS^o (Eq. 64), the computed evaporation rates are extremely sensitive to small changes in the values of these properties. For example, the agreement between theory and experiment may be improved to the degree shown in Fig. 10 by using values for $\Delta H^o_{298.15}$ that do not differ from any of the accepted values by more than the estimated probable error (see Table 2). Even better agreement could be obtained by making minor adjustments in ΔS^o, as well as in ΔH^o, but it is not warranted, because of the limited accuracy of the experimental data[80] and the approximations associated with the model.

Conclusion 1: Results on the temperature dependence of the evaporation rates indicate that, within the degree of accuracy of existing thermodynamic property data, the volatile products are in equilibrium proportions over a wide temperature range if we require equality of the theoretical and experimental values of the over-all evaporation rate of oxygen atoms (if we assume that the rate-limiting step is the equilibration process described by the parameter ζ'_{O_2}).

As an additional test of the present model, it is of interest to determine whether the theoretical results agree with Schissel and Trulson's data on the dependence of the evaporation rates on the chamber pressure, p'_{O_2}. The comparison will be qualitative, not quantitative, since the experimental data on pressure dependence are given in terms of relative pressures, not absolute pressures. The curves shown in Figs. 11-14 were computed for this purpose, but we have chosen to express the results in terms of Z'_{O_2} rather than p'_{O_2} because the impingement rate is a more meaningful parameter in the present treatment than the chamber pressures. Notice in Fig. 11 that the order of the dependence (the slope) of R_O on Z'_{O_2} increases with T, with the upper limit being a first-order dependence, as indicated by a slope of unity. By comparing Figs. 11 and 12, we conclude that the dependence of R_O on Z'_{O_2} becomes first order when Z'_{O_2} is sufficiently low (or T is sufficiently high) that the dissociation of O_2 into O is essentially complete $\left(R_O \approx 2\zeta'_{O_2} Z'_{O_2}\right)$. These characteristics agree with Schissel and Trulson's observation that the order of R_O with respect to Z'_{O_2} increases with T, attaining first order at the highest temperatures where R_O becomes independent of T.

Corresponding results for the dependence of R_{WO_2} on Z'_{O_2} are presented in Figs. 13 and 14. Notice in Fig. 13 that the order (slope) of an isotherm changes rather abruptly from second order to approximately one-third order as Z'_{O_2} increases. It appears that these changes in order occur at values of T and Z'_{O_2} that correspond approximately to the positions of the maxima of R_{WO_2} in Fig. 14, thereby indicating that the order changes at the point where the rate of production of WO_2 is overpowered by a competing reaction. These characteristics agree with Schissel and Trulson's observation that the order of the dependence of R_{WO_2} on Z'_{O_2} increases with T, becoming "at least second order at the highest temperatures."[58]

Conclusion 2: Results on the dependence of R_O and R_{WO_2} on Z'_{O_2} provide evidence that, over a considerable range of conditions, the reaction rates of the adsorbed species are those corresponding to equilibrium kinetics.

A question of practical interest is: How does the rate of erosion of tungsten by oxygen vary with T and Z'_{O_2}? The answer predicted by the present model is illustrated

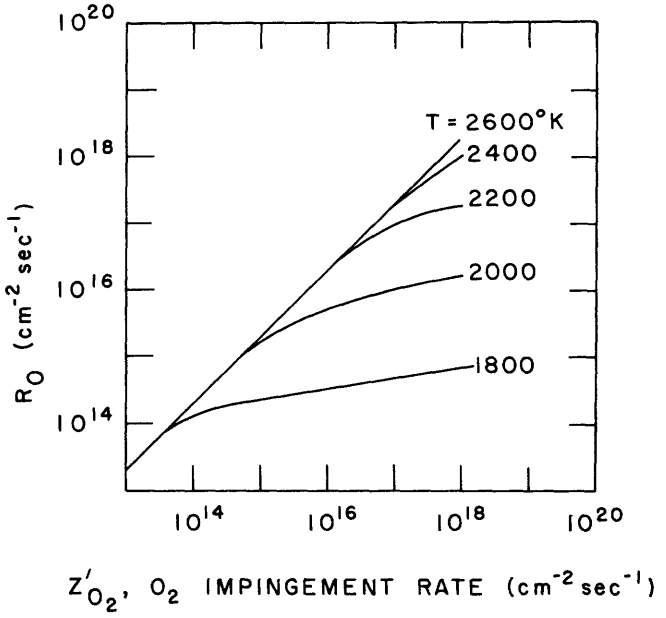

Fig. 11. Theoretical dependence of R_O, the evaporation rate of atomic oxygen, on Z'_{O_2}, the impingement rate of O_2, for various temperatures of the tungsten specimen. As in Fig. 7, the computations are based on tabulated thermodynamic data[76] and on the simplifying assumption that $\zeta'_{O_2} = 1$ over the entire range of conditions.

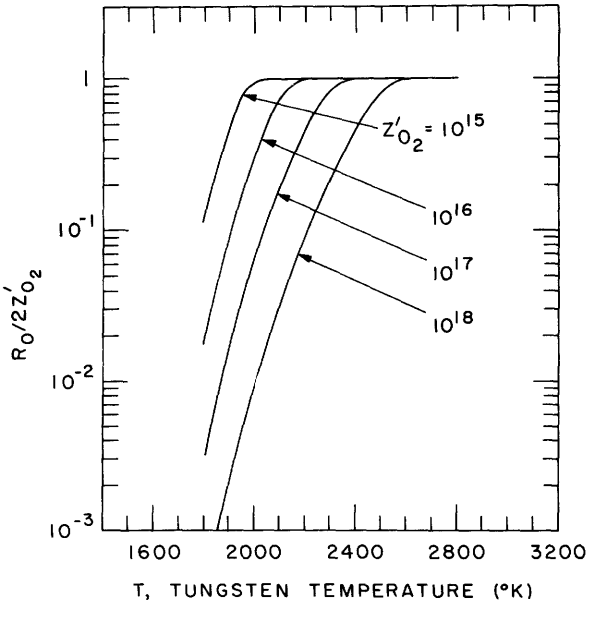

Fig. 12.

Theoretical dependence of R_O, the evaporation rate of atomic oxygen, on T, the temperature of the tungsten specimen, for various values of the impingement rate, Z'_{O_2}. (Assumptions are the same as for Figs. 7 and 11.)

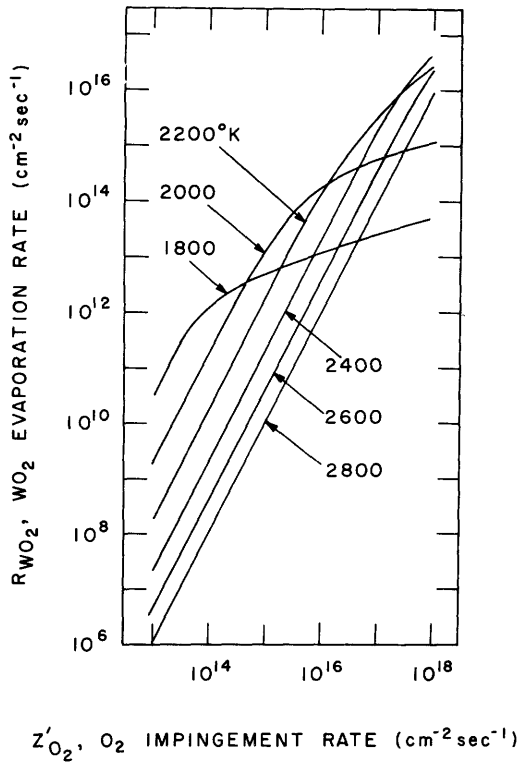

Fig. 13.

Theoretical dependence of R_{WO_2}, the evaporation rate of WO_2, on Z'_{O_2}, the impingement rate of O_2, for various temperatures of the tungsten specimen. (Assumptions are the same as for Figs. 3 and 7.)

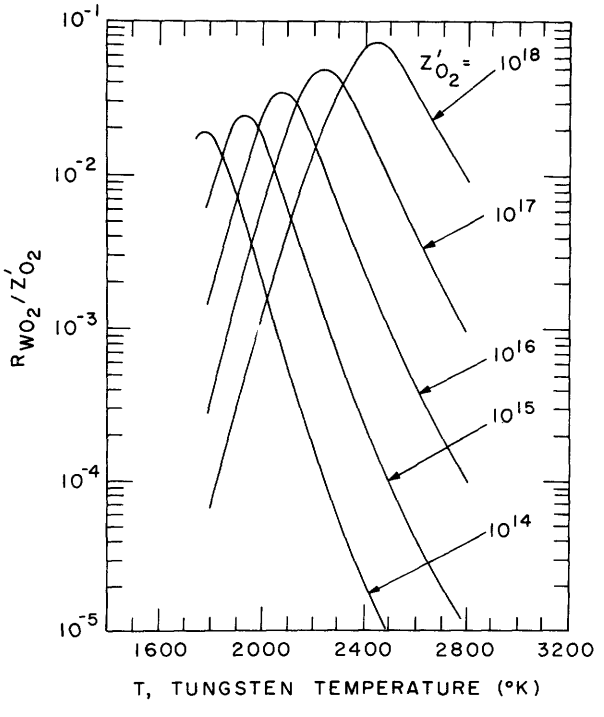

Fig. 14.

Theoretical dependence of R_{WO_2}, the evaporation rate of WO_2, on T, the temperature of the tungsten specimen. (Assumptions are the same as for Figs. 7 and 11.)

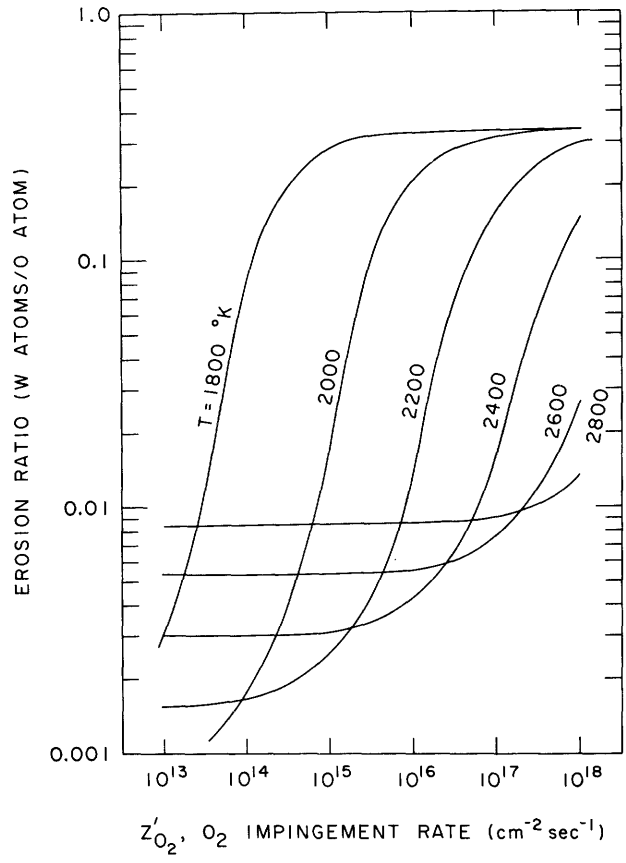

Fig. 15. Theoretical prediction of the average loss of W atoms from the solid per impinging O atom (per 1/2 molecule).(Assumptions are the same as for Figs. 7 and 11.)

in Fig. 15 where the ordinate represents the average number of tungsten atoms removed per impinging oxygen atom (per 1/2 molecule). The results are not expected to be completely realistic because they are based upon the simplifying assumption that ζ'_{O_2} is unity throughout the entire range of conditions. The erosion ratio is ~0.33 at high values of Z'_{O_2} because the dominant volatile species is WO_3 and its polymers. An unusual feature of Fig. 15 is that the erosion ratio for a given impingement rate is not a monotonic function of T, since the formation of WO increases with T as may be seen in Fig. 7. (A detailed comparison of the theoretical predictions with existing experimental data on erosion rates[81] will be given in a subsequent paper.)

D. ANALYSIS AND DISCUSSION OF THE O-Mo REACTION

We also may consider the reaction of oxygen with molybdenum, since both the mass spectrometric data[64] and the necessary thermodynamic property data (Table 3) are available. The results for O-Mo presented in Fig. 16 were computed in the manner described for O-W in the preceding section except that equilibrium constants

Table 3. Thermodynamic property data for the volatile species formed in the reaction of gaseous oxygen with solid molybdenum.

Species	$\Delta H°$ (kcal/gmole)	$\Delta S°$ (cal/gmole-°K)	Reference
O(g)	61.3	16	75
MoO(g)	95	25.5	*
MoO_2(g)	11.0	9.0	*
MoO_3(g)	-80	-15.5	*
Mo_2O_6(g)	-270	-72	*
Mo_3O_8(g)	-400	-118	†
Mo_3O_9(g)	-463	-132	*
Mo_4O_{12}(g)	-640	-190	†

*DeMaria et al.[82] report ΔH_o° (enthalpy at 0°K and 1 atm) for the reactions

$$MoO(g) \rightarrow Mo(s) + O(g)$$
$$MoO_2(g) \rightarrow Mo(s) + 2O(g)$$
$$MoO_3(g) \rightarrow Mo(s) + 3O(g)$$

and free energy functions, $-(F°-H_o^\circ)/T$, at 100° intervals from 2000°K to 2500°K. Burns et al.[83] report $\Delta H°$ and $\Delta S°$ at 1600°K for the reactions

$$2MoO_3(g) \rightarrow (MoO_3)_2(g)$$
$$3MoO_3(g) \rightarrow (MoO_3)_3(g).$$

These data, together with the tabulation of thermodynamic properties[75] of Mo(s), O_2(g), and O(g), have been used to compute, for the particular temperature range of interest, the values of $\Delta H°$ and $\Delta S°$ given in this table.

†Estimated by assuming that the relative magnitudes of the properties for O-Mo follow the same trend as the properties for O-W.

were calculated by using the data of Table 3. The agreement with the experimental data in this case (Fig. 16) is quite similar to that obtained in the previous case (Fig. 7). The apparent equilibration probability for O-Mo is given in Fig. 17, and we see that the results are similar to those for O-W in Fig. 8. The slight shift of ζ'_{O_2} for O-Mo toward lower temperatures than that for O-W is consistent with the fact that both the binding energy[57] and the impingement rate are smaller for O-Mo than for O-W. As may be seen in Fig. 18, the theoretical evaporation rates agree more closely with the experimental data when the apparent equilibration probability is used in place of the assumption that $\zeta'_{O_2} = 1$ over the entire range of conditions.

Conclusion 3: The theoretical model and analysis presented in Section II-C yield results that agree satisfactorily with existing experimental data for O-Mo, as well as

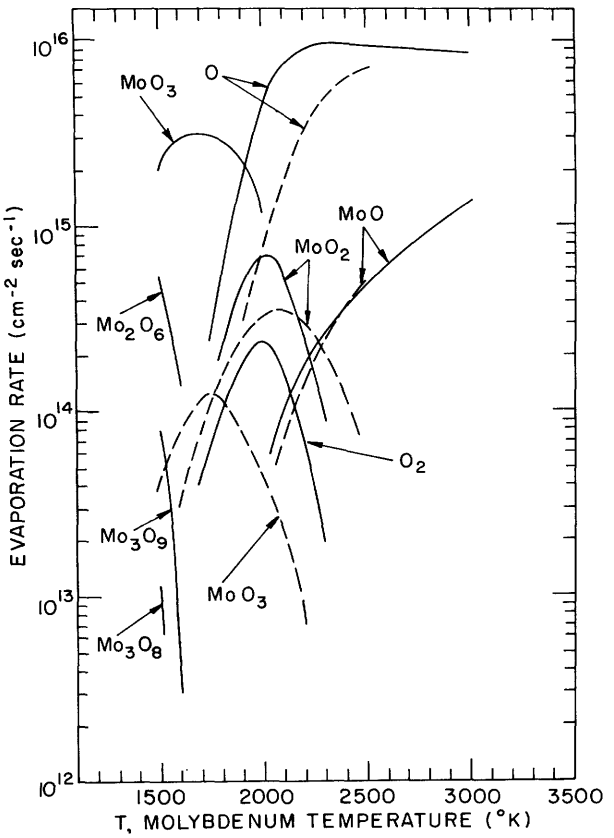

Fig. 16.

Comparison of theoretical evaporation rates with corresponding experimental data of Steele[64] for the chemical reaction of gaseous O_2 with solid molybdenum. The O_2 pressure and temperature are held constant at 5.0×10^{-5} Torr and ~300°K, corresponding to an impingement rate of $Z'_{O_2} = 1.7 \times 10^{16}$ molecules cm^{-2} sec^{-1}. The theoretical results are based on the thermodynamic property data of De Maria et al.[82] and Burns et al.,[83] and on the simplifying assumption that $\zeta'_{O_2} = 1$ over the entire range of conditions.

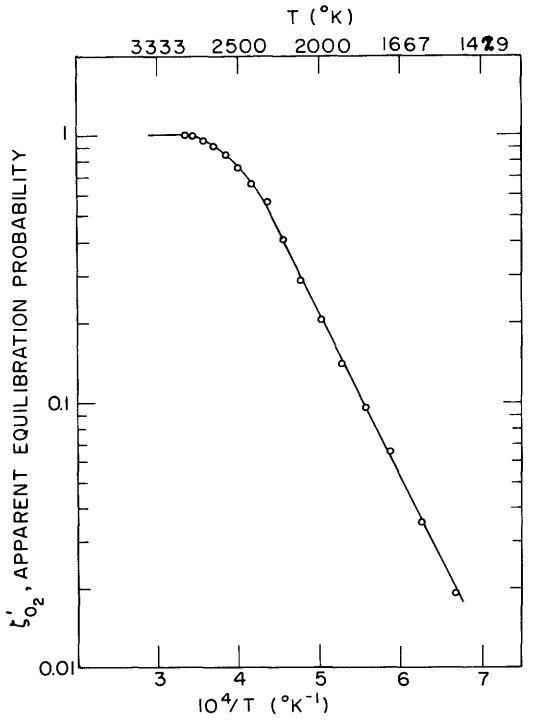

Fig. 17.

Apparent equilibration probability, ζ'_{O_2}, as a function of T, the temperature of the molybdenum specimen. (Calculated from Steele's experimental data by the same method used in connection with Fig. 8.)

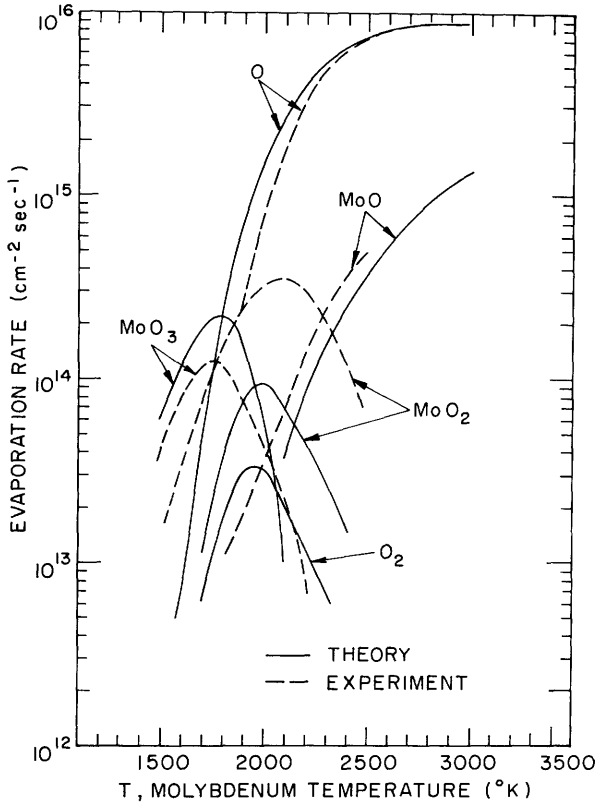

Fig. 18. Comparison of theoretical evaporation rates with corresponding experimental data for the reaction of O_2 with Mo. All conditions and assumptions are identical to those for Fig. 16, except that the computations are based on the equilibration probability shown in Fig. 17, rather than on the assumption that $\zeta'_{O_2} = 1$.

for O-W; therefore, the success of the approach is not limited to a single gas-solid reaction. (Since the properties of Mo and W are quite similar, this does not represent a rigorous test of the generality of the model.)

E. ANALYSIS AND DISCUSSION OF THE O-C REACTION

The reaction of oxygen with carbon is an especially attractive case to study because very accurate data are available[75] on the thermodynamic properties that are needed to compute the equilibrium constants for the expected reactions:

$$C(s) + \tfrac{1}{2} O_2(g) \rightleftharpoons CO(g) \tag{65a}$$

$$C(s) + O_2(g) \rightleftharpoons CO_2(g) \tag{65b}$$

$$C(s) + \tfrac{1}{2} O_2(g) \rightleftharpoons C(s) + O(g). \tag{65c}$$

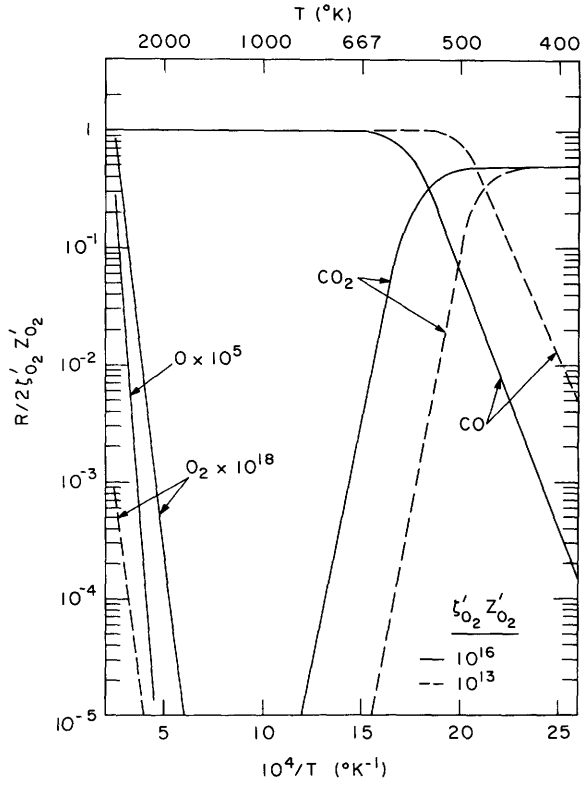

Fig. 19. Theoretical evaporation rates of the volatile species formed in the chemical reaction of gaseous O_2 with solid carbon. It is assumed that $\zeta'_{O_2} = 1$ over the entire range of conditions.

The results presented in Fig. 19 for the graphite phase of carbon have been computed by the method described in Section II-C, under the assumption that $\zeta'_{O_2} = 1$ over the entire range of conditions. The predominant species changes quite abruptly from CO_2 to CO at a temperature that depends only weakly on the impingement rate, Z'_{O_2}. At high temperatures, both R_{CO} and R_O have essentially first-order dependence on Z'_{O_2}, as illustrated in Fig. 19, by the fact that R_{CO}/Σ_O and R_O/Σ_O appear to be independent of Z'_{O_2}. (Note: $\Sigma_O = 2\zeta'_{O_2} Z'_{O_2}$, as in Eq. 59.) The first-order dependence of R_{CO} exists because CO predominates to such a degree at high temperatures that its rate of formation is limited by the impingement rate Z'_{O_2}, rather than by the thermodynamics of the competing reactions. The relation between R_O and R_{CO} is

$$R_O = \frac{\sqrt{7}}{2} \frac{K_O}{K_{CO}} R_{CO}, \tag{66}$$

where K_{CO} and K_O are the equilibrium constants for the reactions described by Eqs. 65a and 65c, respectively, and Eq. 62 has been used to express K_{CO} and K_O in terms of evaporation rates, rather than partial pressures. Since $R_{CO} \propto Z'_{O_2}$, Eq. 66 explains the first-order dependence of R_O on Z'_{O_2} observed in Fig. 19.

Unfortunately, mass spectrometric data of the same calibre as the data for O-W and O-Mo have not yet been reported for O-C, probably because the equilibration probability, ζ'_{O_2}, is so low that the evaporation rates are below the minimum detectable values.[84]

F. CONCLUDING REMARKS

The apparent validity of the present model in two cases, O-W and O-Mo, is quite remarkable, in view of the extreme simplicity of the model. For example, there are possible processes that could invalidate the model: (i) If a detectable fraction of any species (other than O_2) is able to evaporate before being equilibrated to the solid and to the adsorbate,[85] then the volatile products will not be produced in equilibrium proportions and the interaction cannot be considered to comprise only two classes of molecules corresponding to equilibration and nonequilibration, with no chemical reactions occurring in the nonequilibrated class. (ii) The kinetics of formation and evaporation of one or more species may be sufficiently slow that deviations from the equilibrium proportions will occur. In particular, we are surprised that the results indicate that even a large molecule like W_2O_6 is in equilibrium with the other species, in spite of the fact that steric factors associated with adsorbate reactions are expected to differ significantly from those for gas-phase reactions.[86] (iii) In relation to the last statement, we may also expect the equilibration probabilities, ζ_i, of the molecular species to deviate markedly from the assumed value of unity, because of differences in the adsorbate and gas-phase partition functions of a given species.[86] (iv) As illustrated in Part I, the angular distribution of an evaporating species may not have the assumed cosine form if an activation energy of adsorption exists for that species. (v) Since the equilibrium constants employed in the present analysis correspond to the reaction of oxygen with the pure solid substance, rather than with an oxide phase, the approach will not be valid at high pressures and low temperatures where the adsorbate or oxide film is sufficiently thick that the surface behaves more like the bulk oxide than like the pure substance. (The model could be applied to the reaction of oxygen with an oxide surface if the thermodynamic property data needed for determining the equilibrium constants were available.) Other possible limitations of the model are discussed in Section I-F.

With the above-mentioned limitations in mind, the model could also be applied at higher pressures if we based the analysis on continuum fluid mechanics rather than on free-molecule kinetic theory. This modification has not been included because a more rigorous test of the model is possible at low pressures where the effects of gas-phase reactions and transport processes are minimized. Also, we have not yet considered

McKinley's mass-spectrometric data[68,70,72] on various halogen-metal reactions because accurate thermodynamic property data have not yet been found for the gaseous dihalides.

The principal characteristics of the results presented for O-W and O-Mo are (i) the species evaporating from the solid appear to be in complete thermodynamic equilibrium with one another and with the solid, and (ii) the fraction of the impinging molecules that are equilibrated, ζ'_{O_2}, decreases as the adsorbate coverage increases. We expect that the same two characteristics apply to a variety of other gas-solid reactions, as well as to catalytic reactions. Since ζ'_i is the only adjustable parameter in the present approach, we hope that a clearer understanding of the equilibration process will be obtained as a result of both experimental and theoretical investigations.

The advantages of the quasi-thermodynamic approach over the kinetic approach, such as that used by Schissel and Trulson,[59] are that the number of adjustable parameters is less and a model of the adsorbate phase is unnecessary. Also, the validity of the kinetic approach rests in part upon the assumption that the adsorbate may be described in terms of distinct adsorption states and/or species, whereas there is some recent evidence that the states of adsorption and oxidation are indistinguishable.[87]

Part III. Flash Desorption of Oxidation Products from a Tungsten Surface

A. INTRODUCTION

A quasi-equilibrium treatment of heterogeneous reactions was described in Part I, and in Part II this treatment was applied to the chemical reactions of gaseous oxygen with solid tungsten, molybdenum, and carbon under steady-state conditions of low pressure and high temperature. Since the computed rates of evaporation of volatile products were found to agree satisfactorily with existing experimental data for the systems oxygen-tungsten and oxygen-molybdenum, we concluded, although the treatment is based on an oversimplified model, that it may be useful as an approximate description of some gas-solid reactions occurring under steady-state conditions. The objective now is to determine whether the treatment can be modified so that it will also be useful in describing gas-solid reactions occurring for transient conditions such as those encountered in experiments based on the flash desorption technique.

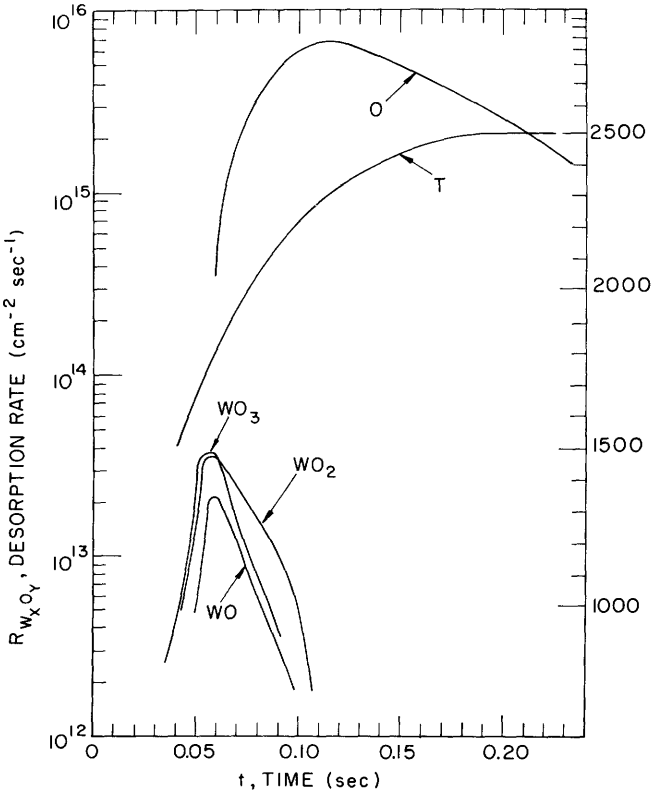

Fig. 20. Experimental flash-desorption curves for the reaction of oxygen with a polycrystalline tungsten surface (Ptushinskii and Chuikov[88]). The mass spectrometric signals for the various species have been converted to an absolute scale of desorption rate by the approximate method described in Appendix C.

Our primary reason for considering the transient case is that the flash desorption technique has been employed recently by Ptushinskii and Chuikov[88] and by McCarroll[29] to obtain detailed data on the reaction of oxygen with tungsten. Since we shall refer frequently to the data of Ptushinskii and Chuikov, it is advantageous to summarize the essential features of their experiment. A polycrystalline tungsten ribbon mounted on a pair of electrical leads was placed inside a vacuum chamber that was generally maintained at an oxygen pressure of $\sim 1 \times 10^{-7}$ Torr. The tungsten temperature, T, was controlled by passing an electric current through the ribbon, and, as illustrated in Fig. 20, this allowed the ribbon to be heated ("flashed") from 300°K to 2500°K in ~0.2 sec, thereby causing oxygen and oxide species to desorb from the surface. A mass spectrometer was positioned immediately in front of the ribbon so that a portion of the species desorbing from the surface passed directly into the ion source of the mass spectrometer without colliding with solid surfaces. The normal procedure was to flash the ribbon only after it had been held at a specific temperature, T_{ad}, sufficiently long to insure that the adsorption of oxygen had reached a steady-state value. The data shown in Fig. 20 are for $T_{ad} = 300°K$, and we see that although atomic oxygen is the predominant species (especially when T rises above 2000°K), the desorption of oxides is significant in the early portion of the flash where the temperature is below 2000°K.

The principal question that we wish to consider is, Can the flash desorption data of Ptushinskii and Chuikov[88] (see Fig. 20) be explained by assuming that the transient reaction is a quasi-static process (that is, a process in which the adsorbate passes through a continuous series of equilibrium states)?

B. THEORETICAL ANALYSIS

The present treatment does not require any assumptions concerning which species exist in the adsorbate phase. Therefore we shall use the symbol [O] to denote the total number of oxygen atoms adsorbed per cm^2 of the tungsten surface, regardless of whether these atoms actually exist as O, O_2, WO, WO_2, etc. Conservation of oxygen requires that d[O]/dt be equal to the difference between the over-all adsorption and desorption rates for oxygen, and, since the adsorption rate is negligible during the flash desorption process of Ptushinskii and Chuikov, we have

$$\sum_x \sum_y y R_{W_xO_y} = -\frac{d[O]}{dt}, \tag{67}$$

where $R_{W_xO_y}$ is the instantaneous value of the desorption rate of species W_xO_y, and the summation includes the principal desorption species. If we assume that the flash desorption process is quasi-static, then the desorption rates of the various species are related through their equilibrium constants which may be expressed as[89]

$$K_{W_xO_y} = (2\pi kT)^{1/2(1-y/2)} \left(\frac{M_{W_xO_y}}{M_{O_2}^{y/2}} \right)^{1/2} \frac{R_{W_xO_y}}{R_{O_2}^{y/2}}, \tag{68}$$

where T is the instantaneous temperature, $M_{W_xO_y}$ is the molecular weight of species W_xO_y, and $K_{W_xO_y}$ represents the equilibrium constant for the general reaction

$$xW(s) + \frac{y}{2} O_2(g) \rightleftharpoons W_xO_y(g). \tag{69}$$

$K_{W_xO_y}$ may be computed from the relation

$$K_{W_xO_y} = \exp\left[-\left(\Delta H^\circ_{W_xO_y} - T\,\Delta S^\circ_{W_xO_y} \right) \Big/ RT \right], \tag{70}$$

where $\Delta H^\circ_{W_xO_y}$ and $\Delta S^\circ_{W_xO_y}$ are the enthalpy and entropy of the reaction described by (69). In the following calculations we shall use the same values of $\Delta H^\circ_{W_xO_y}$ and $\Delta S^\circ_{W_xO_y}$ that resulted in good agreement in Part II (see Table 2).

Since Eq. 68 provides $r-1$ equations in terms of r unknown desorption rates (r = number of species), we must have one more equation in order to obtain a solution. In the following calculations this additional equation will be the graphical representation of the experimental results for R_O vs T shown in Fig. 20. The desorption rate, $R_{W_xO_y}$, may be expressed in terms of R_O by first applying (68) for the case $x = 0$, $y = 1$ (for the formation of atomic oxygen) to obtain a relation between R_{O_2} and R_O, and then using this to eliminate R_{O_2} from (68), the result being

$$R_{W_xO_y} = (2\pi kT)^{1/2(y-1)} \frac{K_{W_xO_y}}{K_O^y} \frac{M_O^{y/2}}{M_{W_xO_y}^{1/2}} R_O^y. \tag{71}$$

We have used the following procedure to compute the desorption rates of the principal oxide species:

1. Choose a value of T and then go to Fig. 20 to determine the corresponding value of R_O.
2. With these values of R_O and T, use Eq. 71 to compute $R_{W_xO_y}$.
3. Repeat steps 1 and 2 for various values of T, thereby obtaining a graph of $R_{W_xO_y}$ vs T (or $R_{W_xO_y}$ vs t, using the T vs t relation shown in Fig. 20).

C. COMPARISON OF THEORETICAL AND EXPERIMENTAL RESULTS

Results obtained by this procedure are presented in Figs. 21 and 22. To simplify the comparison of Fig. 21 with the experimental results in Fig. 20, we have omitted

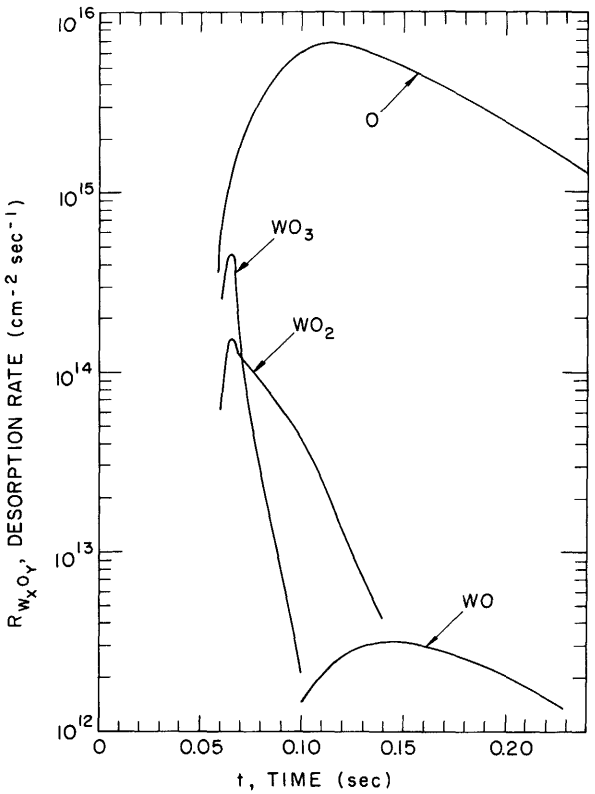

Fig. 21. Theoretical flash-desorption curves for the reaction of oxygen with a tungsten surface. Note: For convenience of comparison with Fig. 20, the curves for those species not appearing in Fig. 20 have been omitted (see Fig. 22).

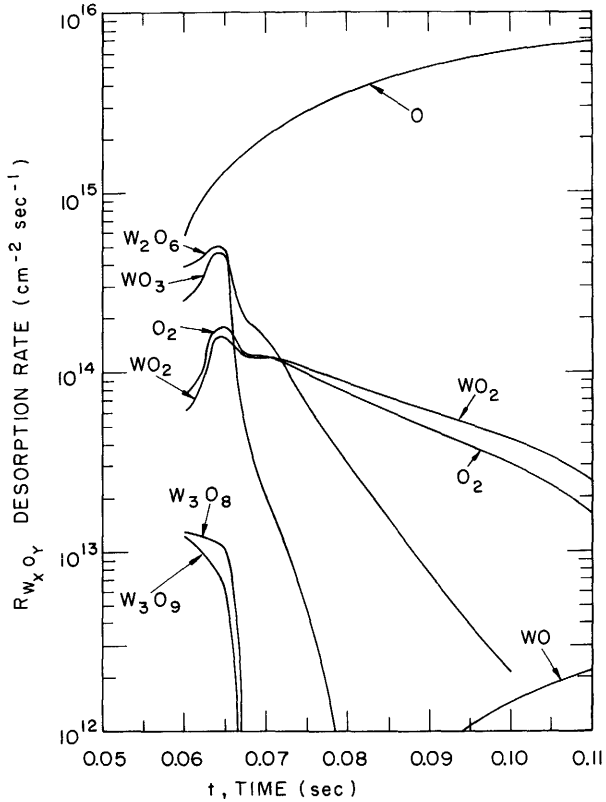

Fig. 22. Theoretical flash-desorption curves for the reaction of oxygen with a tungsten surface. (Conditions are identical to those for Fig. 21, but included here are the results for all of the major species, and the time scale has been enlarged for clarity.)

from Fig. 21 the results for those oxide species that do not appear in Fig. 20. Although our computational procedure forces the curves for O in Figs. 20 and 21 to be identical, it does not force the curves for the other species to agree. In fact, agreement of the curves for a particular species would indicate that the desorption rate for that species equals the "equilibrium" (or quasi-static) value corresponding to the instantaneous values of R_O and T. Notice that the agreement for WO_2 and WO_3 is reasonably good in view of the limited accuracy of both the experimental and theoretical results. (This question of accuracy is considered below.) The lack of agreement for WO is not surprising because the experimental curve is suspected[88] to be the result of electron-impact induced dissociation of WO_2 and WO_3.

The theoretical results for all of the major species are shown in Fig. 22 on an enlarged time scale for clarity. Although the magnitudes of the results for W_2O_6 and O_2 suggest that these species should have been detectable, their absence in the experimental results (Fig. 20) may be due to one or more of the following causes: (i) the O_2 signal was obscured by wall effects,[88] (ii) the equilibrium constant used to calculate the W_2O_6 rate may be erroneous, (iii) the T vs t relation shown in Fig. 20 may not be completely accurate in the range 1500°-2000°K, thereby causing $R_{W_2O_6}$ to be too large,[90] and (iv) the conversion factor used in converting the raw experimental data to the absolute scale of desorption rate shown in Fig. 20 may be slightly high. The importance of point (iv) may be seen in Eq. 71 which predicts that $R_{W_2O_6}$ is proportional to the sixth power of R_O. This point is further illustrated in Fig. 23 which was computed in the following manner. If we assume that the effect of the erroneous conversion factor may be corrected by multiplying the ordinate in Fig. 20 by a constant factor, a, then the corrected value of R_O is a times that shown in the present figure. This corrected value of R_O is used to calculate new results to replace those in Figs. 21 and 22. With these results we calculate both the number of molecules of species W_xO_y desorbed per cm^2 per flash,

$$\int_0^\infty R_{W_xO_y}\, dt \tag{72}$$

and, from (67), the total amount of oxygen desorbed per cm^2 per flash,

$$[O]_o = \sum_x \sum_y \int_0^\infty y\, R_{W_xO_y}\, dt \tag{73}$$

which is numerically equal to $[O]_o$, the oxygen coverage initially on the surface before the flash. Each value of a results in different values of $\int_0^\infty R_{W_xO_y}\, dt$ and $[O]_o$, and the results given in Fig. 23 were obtained by repeating the calculations for a ranging from 0.7 to 1.6. Notice that the amount of W_2O_6 relative to either WO_2 or WO_3 decreases sharply as $[O]_o$ decreases (that is, as a decreases). Since $[O]_o \approx 8 \times 10^{14}$ cm^{-2}

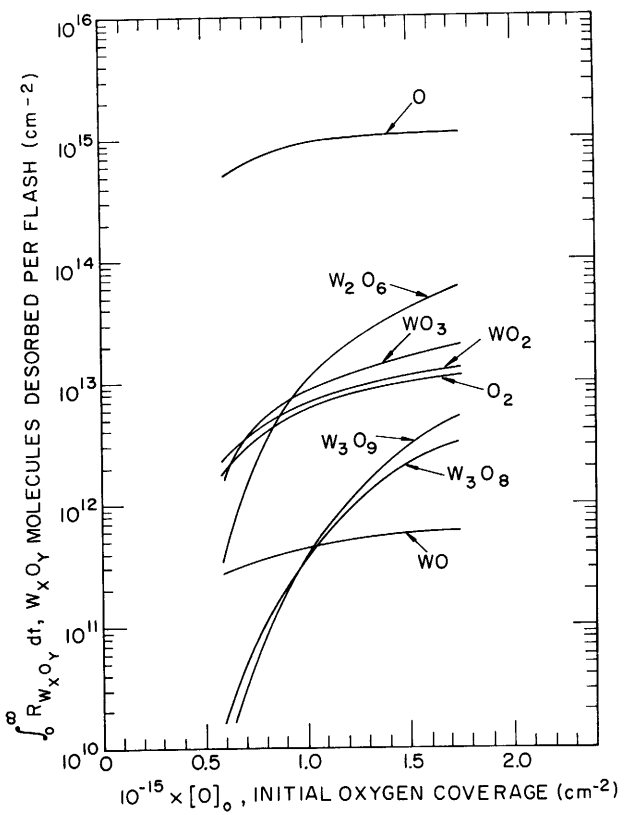

Fig. 23. Theoretical dependence of the amount of each species desorbed per cm^2 per flash on the total amount of oxygen initially adsorbed on the tungsten surface before the flash.

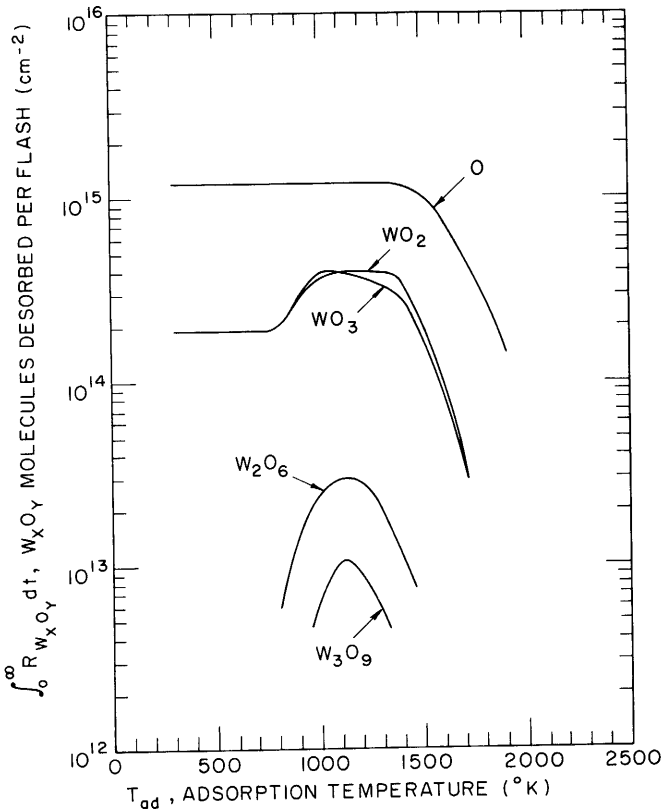

Fig. 24. Experimental results of the effect of adsorption temperature on the amounts of the various species desorbed per cm^2 per flash. (Replotted from Ptushinskii and Chuikov.[88])

for the results shown in Figs. 21 and 22, we conclude from Fig. 23 that the relative amount of W_2O_6 is very sensitive to a small error in the conversion factor used in constructing Fig. 20. (This conversion factor is described in Appendix C.)

Ptushinskii and Chuikov[88] also performed a series of experiments in which they varied T_{ad}, the temperature at which the tungsten ribbon was held during adsorption of oxygen before the flash. These data (Fig. 24) show that $\int_0^\infty R_{W_xO_y}\,dt$, the amount of species W_xO_y desorbed per cm^2 per flash, depends on T_{ad} in a rather complicated manner. Although the amounts of the various species desorbed are seen to be independent of T_{ad} in the range 300°K to ~750°K, the amounts of all species other than O increase markedly if the adsorption process is performed at temperatures in the range $750°K \lesssim T_{ad} \lesssim 1150°K$, thereby indicating an increase in $[O]_o$, the total amount of oxygen adsorbed on the surface before the flash. This increase in $[O]_o$ with T_{ad} has also been reported by other investigators,[91] using different experimental techniques, and the common explanation is that the adsorption of oxygen at high coverages is a thermally activated process. At too high a temperature, however, the adsorbate becomes thermally unstable, thereby causing $[O]_o$ to decrease with increasing T_{ad}, as indicated in Fig. 24 by the fact that the amounts fall off for $T_{ad} > 1250°K$.

If we accept the argument that $[O]_o$ increases with T_{ad} in the range 700°-1150°K, then the theoretical results given in Fig. 23 provide a possible qualitative explanation for the experimental observation (Fig. 24) that the amount of oxygen desorbed as oxides increases in this range, whereas the amount desorbed as O remains essentially

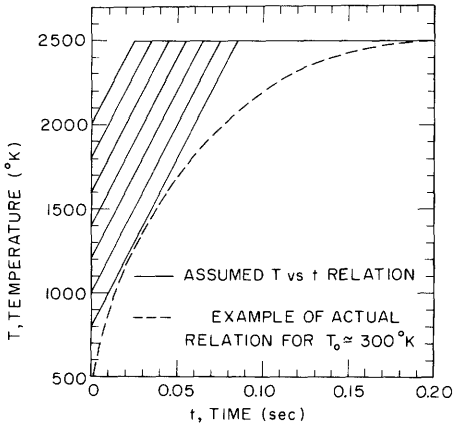

Fig. 25.

Assumed dependence of temperature on time for flash-desorption processes originating at different initial values of T_{ad}, the adsorption temperature immediately preceding the flash. The experimental curve from Fig. 20 is included for comparison.

unchanged. As may be seen in Fig. 23, an increase in $[O]_o$ causes a greater increase in the oxides than in atomic oxygen, especially for $[O]_o > 1 \times 10^{15}$. The results in Fig. 23 are not a suitable basis for making a closer comparison of experimental and theoretical results because they were calculated for $T_{ad} = 300°K$ by using the T vs t relation shown in Fig. 20. Since Ptushinskii and Chuikov[88] do not report the T vs t relations for flashes starting at different values of T_{ad}, we shall base the following

computations on the oversimplified linear relations shown in Fig. 25. Similarly, the lack of experimental data on R_O vs t for different T_{ad} will be compensated for by assuming that R_O may be represented by the expression[92]

$$R_O = kT/h\,[O]\exp(-\chi^*/kT), \tag{74}$$

where k and h are the Boltzmann and Planck constants, respectively, and χ^* is the apparent desorption energy, which is assumed to vary with coverage in the manner shown in Fig. 26. (As described in Appendix D, this approximate relation for χ^* vs [O] was estimated by fitting Eq. 74 to the experimental data.) The final assumption is that the dependence of coverage on adsorption temperature may be approximated by the curve shown in Fig. 27. Using these assumptions we have calculated the curves shown in Fig. 28, which are qualitatively similar to the experimental curves in Fig. 24. The agreement could be improved by slight changes in the assumed relations (Figs. 25-27), but quantitative agreement should not be expected, in view of the numerous oversimplifications and the limited accuracy of the data. (As described in Appendix C, we suspect that the values of $\int_0^\infty R_{W_xO_y}\,dt$ reported by Ptushinskii and Chuikov[88] are too high.)

D. CONCLUDING REMARKS

The development of an atomistic model of the kinetics of the oxygen-tungsten reaction is a formidable task, and at present those concerned with this problem do not even agree on some of the most basic mechanisms. For example, McCarroll's view[93] is that the oxide molecules which desorb from the surface are formed at low temperature before the flash, whereas Ptushinskii and Chuikov[94] question this view and suggest that the oxides may have formed during the flash. Schissel and Trulson[59] have described a kinetic model in which two states of adsorption are assumed. The quasi-equilibrium approach presented here circumvents the problem of formulating an atomistic kinetic model of the reactions among the adsorbate species, and results are obtained without making any assumptions about whether the adsorbate consists of atoms, molecules, radicals, or complexes.

The quasi-equilibrium model provides an extremely simple explanation of the experimental data reported both by Ptushinskii and Chuikov[88] and by McCarroll.[29] The qualitative features of the model may be described most clearly by referring to Eq. 71. Since the term $K_{W_xO_y}/K_O^y$ decreases exponentially[95] with increasing temperature for all of the tungsten oxide species other than WO, it follows that the desorption rates of WO_2, WO_3, W_2O_6, and W_3O_9 will be largest in the low-temperature portion of the flash-desorption process, in agreement with the experimental data shown in Fig. 20. Notice that Eq. 71 also predicts that $R_{W_xO_y}$ is proportional to R_O^y; therefore, since it seems reasonable to expect that R_O increases with increasing oxygen coverage, we conclude

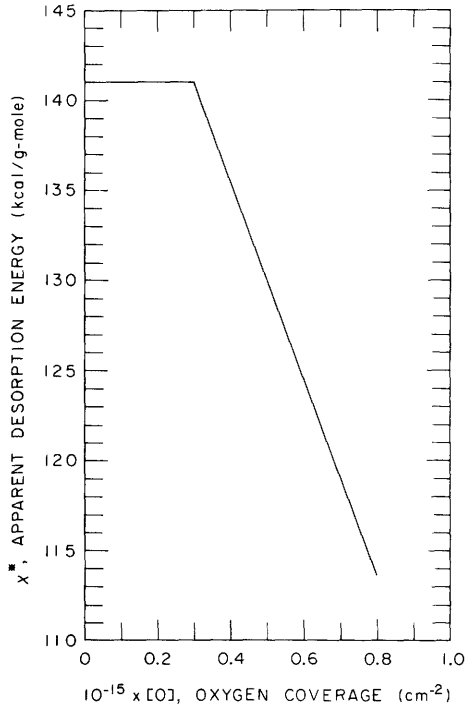

Fig. 26.

Assumed dependence of the apparent desorption energy, χ^*, on oxygen coverage [O]. (This relation has been estimated from Ptushinskii and Chuikov's experimental data[88] by the procedure described in Appendix D.)

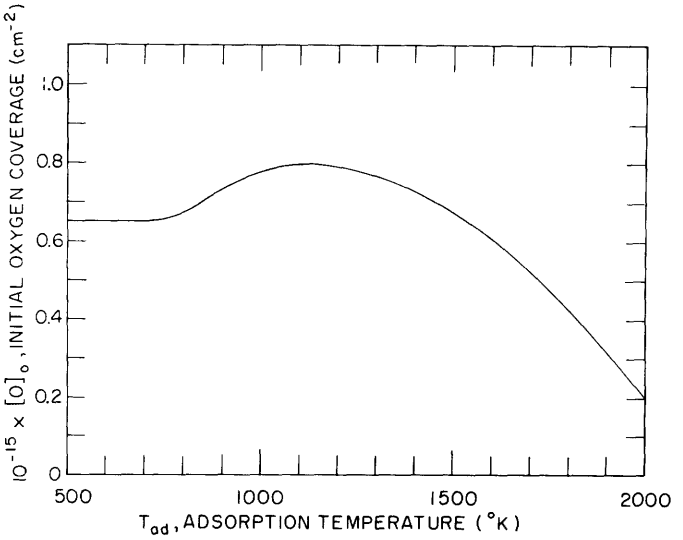

Fig. 27.

Assumed relation for the total amount of oxygen adsorbed at various temperatures. (The qualitative shape of this relation has been estimated from existing experimental data.[88, 91, 59, 100])

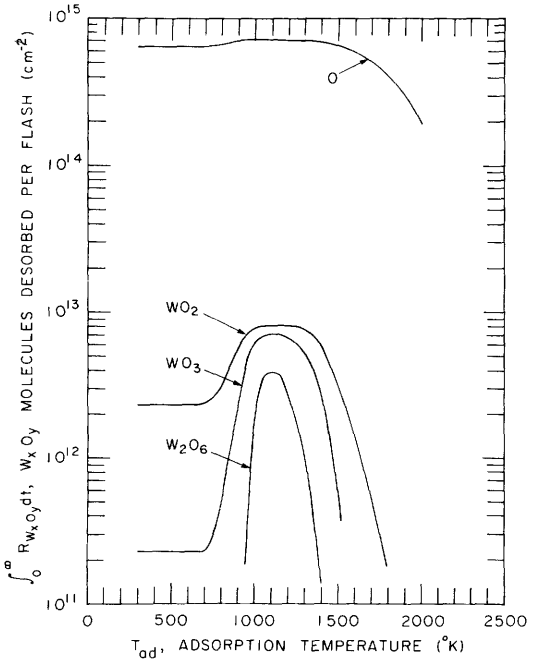

Fig. 28.

Theoretical prediction of the effect of adsorption temperature on the amounts of the various species desorbed per cm^2 per flash.

that the amount of oxides desorbed per flash increases with increasing coverage. This characteristic of the quasi-equilibrium model provides a plausible explanation of the experimental observations that greater amounts of oxides are desorbed per flash when the initial coverage, $[O]_o$, is increased either by increasing the length of the adsorption period[90, 59] or by selecting an adsorption temperature that enhances activated adsorption.[88]

Since the results of the quasi-equilibrium analysis agree, at least qualitatively, with both the steady-state and flash-desorption experimental data, we have reasonable support for the idea that the desorption process of the oxygen-tungsten reaction does not deviate radically from being a quasi-static process. That is, both the rates of the reactions occurring within the adsorbate phase and the rates of desorption of the various species are sufficiently rapid that the desorbing species remain in chemical equilibrium with one another, even for transient conditions in which T and [O] are varying with time.

Since the validity of the quasi-equilibrium approach is limited by a number of factors (see Section II-F), we cannot expect it to apply for all experimental conditions and gas-solid systems. It does, however, provide a useful standard for determining the degree to which a process deviates from being quasi-static. The nature of the deviation may then serve as a guide to identifying the rate-controlling mechanism and developing an improved kinetic model. For example, this approach may prove to be useful in developing an explanation for the most recent data of Ptushinskii and Chuikov,[96] which indicates that the flash-desorption rates for the oxygen-tungsten system depend on the crystallographic orientation of the surface. The approach may also be applied to catalytic reactions, and work in this direction is now in progress.

APPENDIX A

Application of Detailed Balancing Considerations to Gas-Solid Interaction Processes

As defined in Section I-B, ${}^3Z$ represents the rate at which gas particles having speeds within the range v to v + dv and directions with the solid angle $d\omega = \sin\theta\, d\theta d\phi$ impinge upon a surface element of unit area. In order to preserve equilibrium conditions,[43] there must be an equal rate (${}^3\beth$) of particles leaving the surface in the reverse direction within the same ranges of v and ω. That is,

$$ {}^3\beth(v, \theta, \phi; T, p) = {}^3Z(v, \theta, \phi; T, p), \tag{A. 1} $$

where the temperature and pressure, T and p, determine the thermodynamic state of the system, and v, θ, and ϕ determine a particular microstate of the free particles.

Assume for the moment that ${}^3\beth$ may be expressed as the sum of two distinguishable components,

$$ {}^3\beth = {}^3R + {}^3R^*, \tag{A. 2} $$

where ${}^3R$ is the rate at which equilibrated particles from all possible adsorbed states contribute to the population of microstate (v, θ, ϕ), and ${}^3R^*$ is the rate at which nonequilibrated particles are scattered into microstate (v, θ, ϕ) from all possible microstates of the impinging gas particles. The emission probability ${}^3\xi$ may be defined as

$$ {}^3\xi = {}^3R/{}^3\beth = {}^3R/{}^3Z. \tag{A. 3} $$

Since the impingement rate per unit solid angle, ${}^3Z/d\omega$, varies as $\cos\theta$ according to Eq. 9, it follows from Eq. A. 1 that ${}^3\beth/d\omega$ also varies as $\cos\theta$. Therefore, if the desorption rate per unit solid angle, ${}^3R/d\omega$, varies as $\cos\theta$ (as is commonly assumed), then Eqs. A. 2 and A. 3 lead to the conclusions that ${}^3R^*/d\omega$ varies as $\cos\theta$, whereas ${}^3\xi/d\omega$ is independent of θ. By a similar argument we can prove that if the equilibrated particles desorbing from the surface have a Maxwellian speed distribution, then the nonequilibrated particles must also have a Maxwellian distribution.

In an analogous manner, assume that ${}^3Z$ may be expressed as the sum of two distinguishable components,

$$ {}^3Z = {}^3\Gamma + {}^3\Gamma^*, \tag{A. 4} $$

where ${}^3\Gamma$ is the rate of collisions that result in equilibration of gas particles to the solid, and ${}^3\Gamma^*$ is the rate of the remaining (nonequilibrated) collisions. The equilibration probability ${}^3\zeta$ is defined as

$$ {}^3\zeta = {}^3\Gamma/{}^3Z. \tag{A. 5} $$

Equations A. 2 through A. 5 may be applied only if we can devise a method for distinguishing the equilibrated particles from the nonequlibrated ones. Since detailed information of this sort is beyond the capabilities of thermodynamics, we are forced to adopt a mechanical approach based on an assumed model of the interaction. For example, if a model enables one to define a boundary in phase space that effectively separates the states of equilibrated adsorbed particles from those of free particles, then this boundary may be used to distinguish equilibrated particles from nonequilibrated particles. That is, ${}^3R$ may be defined as the differential rate at which particles cross the boundary from all possible adsorption states to populate the free state (v, θ, ϕ), whereas ${}^3\Gamma$ is the rate of the reverse process. The principle of detailed balance[44] may be applied at the boundary to give

$$ {}^3R = {}^3\Gamma \tag{A.6} $$

at equilibrium. This result may be combined with Eqs. A. 2-A. 5 to prove that

$$ {}^3\xi = {}^3\zeta \tag{A.7a} $$

and

$$ {}^3R^* = {}^3\Gamma^*. \tag{A.7b} $$

We emphasize the fact that Eqs. A. 6 and A. 7 are not valid if the boundary does not provide a definite separation between the adsorbed and free states; for example, if it does not ensure that a negligible fraction of the free particles entering the adsorbed state reside for so short a time that they return to the free state before being equilibrated to the solid.

The model of dissociative adsorption employed in Section I-F is an example of the approach described above, and in that case either the dashed curve or the dot-dash curve in Fig. 3 is a possible choice of the boundary separating the adsorbed and free states. Although the dashed curve appears to be a more appropriate choice than the dot-dash curve for transitions from free to adsorbed states, the reverse is true for transitions in the opposite direction; therefore, as a compromise we could choose a vertical line passing through the activation barrier E_a as the boundary. (Because of the exponential nature of the equilibrium energy distribution function, the results for the three different choices of boundaries will be essentially the same in most cases.) The results of Section I-E show that, for the assumed model, the dependence of ${}^3R$ on v is not Maxwellian, and the dependence of ${}^3R/d\omega$ is not $\cos\theta$.

APPENDIX B

Relation of the Quasi-Equilibrium Model to the Statistical Theory of Chemical Reaction Rates

The purpose of this appendix is to demonstrate that the quasi-equilibrium treatment of heterogeneous reactions may be formulated in a manner similar to the statistical theory of homogeneous reactions. Although the statistical theory is formally applicable to any homogeneous reaction, Keck[45] developed it explicitly for the recombination process

$$A + B + C \rightleftharpoons AB + C \tag{B. 1}$$

where the "catalyst," C, is a gaseous species that does not react with either A or B. By analogy, we shall extend the formalism of the statistical theory to the reaction

$$A + B + M \rightleftharpoons AB + M, \tag{B. 2}$$

where the catalyst, M, is a solid surface that is assumed not to form volatile products, such as AM or BM, at the temperatures and pressures of interest.

We shall begin by reviewing the application of the statistical theory to the reaction described by Eq. B. 1 which may be expressed as

$$A + B + C \rightleftharpoons (ABC)^* \rightleftharpoons AB + C, \tag{B. 3}$$

where $(ABC)^*$ denotes the "collision complex." To obtain an expression for the recombination rate, R_{fb}, we consider the steady-state flow of representative points in phase space from the "free state," A + B + C, through the "collision complex," $(ABC)^*$, to the "bound state," AB. From this point of view, the recombination rate may be written[45]

$$R_{fb} = \iiint_{R_{f*}\epsilon_{*b}>0} R_{f*}(P, L, E)\, \epsilon_{*b}(P, L, E)\, dP dL dE, \tag{B. 4}$$

where $R_{f*}(P, L, E)$ is the rate at which $(ABC)^*$ is formed by collisions of A + B + C having total linear momentum, P, total angular momentum, L, and total energy, E, and $\epsilon_{*b}(P, L, E)$ is the probability of such collisions resulting in the formation of the bound state, AB. Because of the difficulty of calculating ϵ_{*b} from first principles, the problem is to devise a means for estimating ϵ_{*b}. The fundamental assumption of the statistical theory is that the collisions randomize the systems to the degree that, subject to known conservation laws, the density in phase space of systems leaving the collision complex is uniform, independent of the initial density of systems entering.[45] This assumption allows us to write ϵ_{*b}[45]

$$\epsilon_{*b}(P,L,E) = \Gamma_{*b}(P,L,E)/[\Gamma_{*b}(P,L,E) + \Gamma_{*f}(P,L,E)], \tag{B.5}$$

where $\Gamma_{*b}(P,L,E)$ and $\Gamma_{*f}(P,L,E)$ are the rates of flow of phase volume per unit P, L, and E from the collision complex to the bound and free states, respectively. That is, ϵ_{*b} is the fraction of the flow that goes to the bound state, and it may be calculated by integrating the phase volume flow over the boundary of the region $(ABC)^*$ in phase space.

If the catalyst is a solid rather than a gaseous species, then the preceding formalism must be modified to account for the fact that the adsorbate phase is not a perfect analog of the collision complex, $(ABC)^*$. One difference is that, whereas $(ABC)^*$ consists of one atom each of A, B, and C, the adsorbate consists of a collection of atoms A, B, and M. Since the composition of the adsorbate varies with the magnitudes of the rates at which A and B impinge upon the surface, we conclude that composition is now a variable whereas it was a constant for the collision complex of homogeneous reactions. To simplify this discussion, we shall take species B to be identical to species A, and the reaction will be expressed in the form

$$A + A + M \rightleftharpoons (AM)^a \rightleftharpoons A_2 + M \tag{B.6}$$

where $(AM)^a$ represents the adsorbate phase. We shall also assume that steady-state conditions exist. Since the process leading from the free state, A + A + M, through the adsorbate phase, $(AM)^a$, to the bound state, A_2, is even more complex than that for the corresponding homogeneous reaction, we shall not attempt to consider the mechanics of the interaction in detail. Instead, we shall make the following assumption which is consistent with the spirit of the statistical theory: The rates at which atoms and molecules leave the adsorbate phase are identical to the equilibrium rates, subject to the conservation relation

$$\Sigma' = 2R_{A_2} + R_A, \tag{B.7}$$

where Σ' is the total rate at which A enters the adsorbate (that is, the atomic rate plus twice the molecular rate), and R_A and R_{A_2} are the equilibrium rates at which atoms and molecules leave the adsorbate. This is equivalent to assuming that the adsorbate is in an equilibrium state determined by the catalyst temperature, T, and the adsorption rate,[46] Σ', and it allows us to express ϵ_{ab} as

$$\epsilon_{ab}(T,\Sigma') = 2R_{ab}(T,\Sigma')/[2R_{ab}(T,\Sigma') + R_{af}(T,\Sigma')]. \tag{B.8}$$

These rates may be calculated by equating R_{ab} to R_{ba} and R_{af} to R_{fa} on the basis of the principle of detailed balance (Eqs. 15 and A.6), and combining the conservation relation (Eq. B.7) and the equilibrium constant (Eq. 43) to obtain

$$R_{af} = \frac{1}{4}(\pi m_A kT)^{-1/2} K_p^2 \left[-1 \pm \left[1 + 8(\pi m_A kT)^{1/2} K_p^{-2} \Sigma'\right]^{1/2}\right] \tag{B.9}$$

and

$$R_{ab} = \frac{1}{2}(\Sigma' - R_{af}). \tag{B.10}$$

Σ' may be expressed either in terms of momentum, as in the statistical theory, or in terms of v, θ, and ϕ, as in Section I-B. Using the latter approach and the nomenclature defined in the present report, we may express the differential rate at which A enters the adsorbate from both free and bound states as

$$^3\Sigma' = 2\,{}^3\zeta'_{A_2}\,{}^3Z'_{A_2} + {}^3\zeta'_A\,{}^3Z'_A, \tag{B.11}$$

where the equilibration probabilities ζ'_{A_2} and ζ'_A are functions of v, θ, ϕ, Σ', and T. (In the language of the statistical theory, $^3\zeta'_{A_2}$ and $^3\zeta'_A$ correspond to ϵ_{ba} and ϵ_{fa}, respectively. A parameter similar to $^3\zeta'$ also appears in homogeneous reactions if there is an activation energy (for example, a rotational barrier) associated with forming the collision complex.) Therefore, the recombination rate may be written

$$R_{fb} = \int_{\phi=0}^{2\pi}\int_{\theta=0}^{\pi/2}\int_{v=0}^{\infty} {}^3\zeta'_A\,{}^3Z'_A\epsilon_{ab}\,dvd\theta d\phi, \tag{B.12}$$

which is similar in form to Eq. B.4 for the corresponding homogeneous reaction. According to the present model, however, ϵ_{ab} is independent of v, θ, and ϕ, so it may be taken outside the integral, giving

$$R_{fb} = \epsilon_{ab}\zeta'_A Z'_A, \tag{B.13}$$

where

$$\zeta'_A Z'_A = \int_{\phi=0}^{2\pi}\int_{\theta=0}^{\pi/2}\int_{v=0}^{\infty} {}^3\zeta'_A\,{}^3Z'_A\,dvd\theta d\phi. \tag{B.14}$$

In summary, we have demonstrated that the quasi-equilibrium model for heterogeneous reactions may be formulated along lines similar to those of the statistical theory for homogeneous reactions. The principal differences of the treatments of heterogeneous and homogeneous reactions arise from the fact that an adsorbate phase is not completely analogous to a collision complex. The collision complex is a particular unstable species, while the adsorbate is a stable phase consisting of a variety of species. In principle, the adsorbate itself could be considered as a collection of collision complexes that lead to desorption of atoms and molecules. In practice, however, rigorous theoretical treatments of adsorbate kinetics are even more complex than for gas-phase kinetics. As a result, our treatment of heterogeneous reactions tends to lean more

toward a phenomenological approach than does the statistical theory of homogeneous reactions. This difference causes ϵ_{ab} (Eq. B. 8) to be a function of macroscopic parameters, T and Σ', whereas ϵ_{*b} (Eq. B. 5) is a function of mechanical parameters. Although the treatment of heterogeneous reactions does not provide as detailed a description as that for homogeneous reactions, we suggest that the fundamental assumption of the statistical approach is a better approximation in the former case than in the latter because the adsorbate may be more effective than a collision complex in randomizing the states of a system.

APPENDIX C

Approximate Method for Converting Mass Spectrometric Data to Desorption Rates

In order to compare our theoretical results with the experimental data of Ptushinskii and Chuikov[88] it was necessary to adopt an approximate method for relating their mass spectrometric data to an absolute scale of desorption rate. The governing relation for a spectrometer having a through-flow ion source is[97]

$$R_{W_xO_y} = \Lambda \left(\frac{T}{M_{W_xO_y}} \right)^{1/2} \frac{I_{W_xO_y}}{\sigma_{W_xO_y} \gamma_{W_xO_y} \iota_{W_xO_y}}, \qquad (C.1)$$

where $R_{W_xO_y}$ is the evaporation rate of species W_xO_y expressed as molecules per sec, Λ is a proportionality constant, T is the temperature of the evaporated molecules (that is, the temperature of the tungsten specimen), $I_{W_xO_y}$ is the mass spectrometer output signal (ion current) corresponding to singly charged positive ions having molecular weight $M_{W_xO_y}$, $\sigma_{W_xO_y}$ is the ionization cross section of W_xO_y, $\gamma_{W_xO_y}$ is the average number of secondary electrons produced per W_xO_y ion at conversion dynode of the electron multiplier,[97] and $\iota_{W_xO_y}$ is the isotropic abundance factor for the particular isotope of W_xO_y having molecular weight $M_{W_xO_y}$. Since the current and energy of the ionizing electrons are held constant, they have been included in Λ. The principal assumptions underlying the application of Eq. C.1 to Ptushinskii and Chuikov's data are the following:

1. It is assumed that all of the species evaporate with a Maxwellian velocity distribution having temperature equal to the instantaneous value of the tungsten ribbon. This assumption has two consequences: (a) the average speeds of the various species in the ion source will be proportional to $\left(T/M_{W_xO_y} \right)^{1/2}$; (b) the spatial distributions of all evaporating species will be identical, i.e., diffuse. [If the spatial distributions of one or more species were not diffuse, as is possible for some activation barriers,[37] then it would be necessary to account for this effect in Eq. C.1.]

2. The approximation of Otvos and Stevenson[98] is used to estimate the ionization cross sections of the volatile species, and no attempt is made to account for the fact that the dependence of σ on electron energy is not the same for all species.[97]

3. Although it is known that the magnitude of γ depends upon the species,[97] we assume for simplicity that γ is a constant.

4. It is assumed that the mass spectrometric data reported by Ptushinskii and Chuikov are for the most abundant isotope of each chemical species.

5. The time that it takes an evaporated molecule to travel from the tungsten

surface to the ion source is negligible relative to the flash-desorption time scale shown in Fig. 20.

With these assumptions we obtain the following equations in which Λ now includes γ:

$$R_O = 7.6 \times 10^{-2}\, \Lambda T^{1/2} I_O \tag{C.2a}$$

$$R_{WO} = 3.45 \times 10^{-3}\, \Lambda T^{1/2} I_{WO} \tag{C.2b}$$

$$R_{WO_2} = 3.17 \times 10^{-3}\, \Lambda T^{1/2} I_{WO_2} \tag{C.2c}$$

$$R_{WO_3} = 2.93 \times 10^{-3}\, \Lambda T^{1/2} I_{WO_3}. \tag{C.2d}$$

We see, therefore, that the conversion from ion currents to evaporation rates may be accomplished if Λ is known. Unfortunately, Ptushinskii and Chuikov did not determine Λ directly from measurements of the sublimation rate of tungsten, which is accurately known.[99]

The procedure that we have used to estimate Λ is based on the relation

$$[O]_o = \sum_x \sum_y y \int_0^\infty R_{W_xO_y}\, dt, \tag{C.3}$$

where $[O]_o$ is the total number of O atoms adsorbed per cm^2 of surface area prior to the flash (at t = 0), $\int_0^\infty y R_{W_xO_y}\, dt$ represents the number of O atoms removed from the surface as W_xO_y molecules, and the summation is over the principal species. Since Eq. C.2 may be substituted for $R_{W_xO_y}$, the integrals appearing in Eq. C.3 may be evaluated by graphically integrating Ptushinskii and Chuikov's data (Fig. 3 in ref. 88) after replotting it in the form $T^{1/2} I_{W_xO_y}$ against t. The results obtained are

$$\int_0^\infty R_O\, dt = 1.95 \times 10^4\, \Lambda \tag{C.4a}$$

$$\int_0^\infty R_{WO}\, dt = 13\, \Lambda \tag{C.4b}$$

$$\int_0^\infty R_{WO_2}\, dt = 34\, \Lambda \tag{C.4c}$$

$$\int_0^\infty R_{WO_3}\, dt = 24\, \Lambda. \tag{C.4d}$$

By substituting these in Eq. C.3 and solving for Λ, we obtain

$$\Lambda = 5.1 \times 10^{-5} [O]_o. \qquad (C.5)$$

Although the exact value of $[O]_o$ is not known, there is experimental evidence[88, 91, 96, 57] that $10^{14} < [O]_o < 10^{16}$. Therefore, Eq. C.5 enables us to estimate Λ on the basis of a reasonable estimate of $[O]_o$. The results shown in Fig. 20 are for $[O]_o \approx 8 \times 10^{14}$.

Instead of employing a procedure similar to that described above, Ptushinskii and Chuikov chose to estimate the conversion factor from experimental data obtained by three independent techniques[1]: (i) a quartz-crystal microbalance was used to determine the mass of tungsten oxide desorbed in a known number of flashes; (ii) measurements of the transient decrease in O_2 pressure caused by adsorption provided an estimate of $[O]_o$, the total number of O atoms adsorbed at a specific temperature, T_{ad}; (iii) flash desorption data, such as those replotted in Fig. 20, were used as the basis for assuming that approximately equal amounts of WO_2 and WO_3 are desorbed in a flash from $T_{ad} = 300\,°K$. By combining these results, Ptushinskii and Chuikov estimated that $\sim 1.2 \times 10^{15}$ O atoms, $\sim 1.9 \times 10^{14}$ WO_2 molecules, and $\sim 1.9 \times 10^{14}$ WO_3 molecules desorb per cm^2 of tungsten surface in a flash from $T_{ad} = 300\,°K$. The value of $[O]_o$ computed from these figures is 2.15×10^{15} cm^{-2}, and by substituting this in our procedure (Eqs. C.5 and C.4), we may compute that $\sim 2.13 \times 10^{15}$ O atoms, $\sim 3.7 \times 10^{12}$ WO_2 molecules, and $\sim 2.6 \times 10^{12}$ WO_3 molecules desorb per cm^2 per flash. Since we believe that the deviation of these values from those of Ptushinskii and Chuikov is too large to be ascribed to the uncertainties associated with our procedure, we suggest that the experimental data on which their conversion procedure is based may be inaccurate. This suggestion is supported by McCarroll's conclusion[29] based on similar flash desorption data that the amounts of WO_2 and WO_3 molecules desorbed per flash are less than 1% of the amount of O atoms desorbed. Since Ptushinskii and Chuikov's flash desorption data are consistent[101] with McCarroll's data before applying conversion procedures, we have reason to believe that the portion of their data which we use in this report is reliable.

APPENDIX D

Estimate of the Desorption Energy of Atomic Oxygen on Tungsten for Varying Coverage

Although we do not expect that Eq. 74 is a valid expression for R_O except in the limit of zero coverage, we shall apply it at higher coverages also, with the understanding that χ^* represents an apparent desorption energy rather than the true desorption energy. The following procedure is employed here to estimate the dependence of χ^* on [O] from Ptushinskii and Chuikov's experimental data for R_O shown in Fig. 20.

Let $R_O(t_1)$ and $R_O(t_2)$ represent the atomic oxygen desorption rates at times t_1 and t_2, respectively, where $t_2 = t_1 - \Delta t$. If Δt is small, then the rate of change of the oxygen coverage may be approximated by

$$\frac{d[O]}{dt} \approx \frac{[O(t_1)] - [O(t_2)]}{\Delta t} \tag{D.1a}$$

$$\approx \frac{R_O(t_1) - R_O(t_2)}{\Delta t} \frac{h}{kT} \exp\left[\frac{\chi^*}{kT}\right], \tag{D.1b}$$

where Eq. 74 has been used to replace [O] by $R_O(h/kT)\exp(\chi^*/kT)$. A second expression is obtained from the fact that d[O]/dt is approximately equal to the average desorption rate,

$$\frac{d[O]}{dt} \approx -\frac{1}{2}[R_O(t_1)+R_O(t_2)]. \tag{D.2}$$

By equating Eqs. D.1b and D.2 and then solving for χ^*, we obtain

$$\chi^* = kT \ln\left[-\frac{\Delta t}{2}\frac{kT}{h}\frac{R_O(t_1) + R_O(t_2)}{R_O(t_1) - R_O(t_2)}\right]. \tag{D.3}$$

Once χ^* is known, Eq. 74 may be used to compute the value of [O] at $t = \frac{1}{2}(t_1+t_2)$. We have applied this procedure to the curve for R_O in Fig. 20, and the results are presented in Fig. 29. (Since both T and χ^* vary quite strongly with time in the initial portion of the flash, we have used a small time increment. The contributions of WO, WO_2, and WO_3 to [O] have been neglected because they are small relative to the contribution due to O.)

According to the results shown in Fig. 29, χ^* attains a constant value of 141 kcal (6.1 eV) in the limit of zero coverage. Since the desorption rates appear only as a ratio in Eq. D.3, the procedure for determining χ^* is independent of the conversion factor used in converting the mass spectrometric readings to the absolute scale of desorption rate in Fig. 20. Therefore, the present result for χ^*

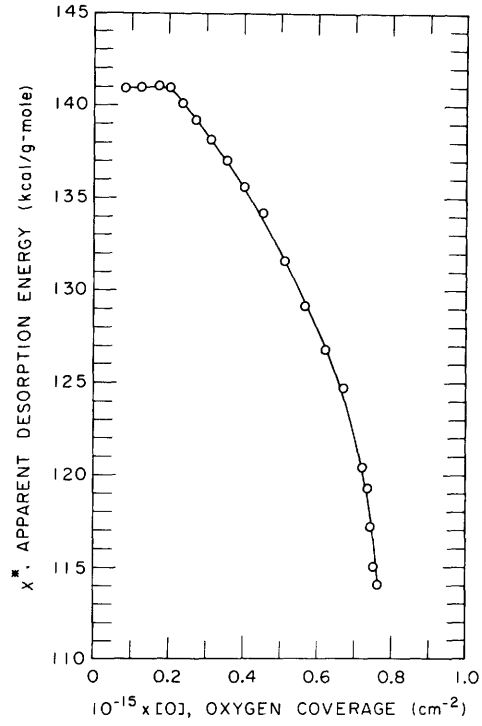

Fig. 29. Dependence of the apparent desorption energy, χ^*, on oxygen coverage, [O]. (These results were calculated from Ptushinskii and Chuikov's experimental data shown in Fig. 20.)

at low coverages agrees with that computed by Ptushinskii and Chuikov[88] (~6 eV) from the same data. As may be seen in Table I of Engelmaier and Stickney,[57] a desorption energy of ~6 eV is consistent with the results of several other experimental investigations of oxygen on tungsten.

References

1. O. Knackle and I. N. Stranski, in Progress in Metal Physics, Vol. 6 (Macmillan Company, New York, 1956).
2. J. P. Hirth and G. M. Pound, Condensation and Evaporation – Nucleation and Growth Processes, Progress in Materials Science Monograph (Pergamon Press, New York, 1963).
3. O. W. Richardson, The Emission of Electricity from Hot Bodies (Longmans, Green, and Company, 2d edition, 1921), Chap. 2.
4. C. Herring and M. H. Nichols, Rev. Mod. Phys. 21, 185 (1949).
5. M. D. Scheer and J. Fine, J. Chem. Phys. 42, 3645 (1965); 46, 3998 (1967); 47, 4267 (1967); and in Proc. Fourth International Materials Symposium, Berkeley, California (in press).
6. E. Ya. Zandberg, N. I. Ionov, and A. Ya. Fontegode, Soviet Phys. – Tech. Phys. 10, 1164 (1966).
7. I. Langmuir and K. H. Kingdon, Proc. Roy. Soc. (London) A107, 61 (1925). For a recent review, see M. Kaminsky, Atomic and Ionic Impact Phenomena on Metal Surfaces (Academic Press, New York, 1965), Chaps. 8 and 9.
8. I. Langmuir, J. Am. Chem. Soc. 38, 1145 (1916); G. E. Review 29, 153 (1926).
9. G. Ehrlich, J. Chem. Phys. 31, 1111 (1959).
10. D. Brennan, in Advances in Catalysis, Vol. 15 (Academic Press, New York, 1965), pp. 1-30.
11. For example, see B. Bergsnov-Hansen and R. A. Pasternak, J. Chem. Phys. 45, 1199 (1966); G. E. Moore and F. C. Unterwald, J. Chem. Phys. 48, 5378 and 5393 (1968); T. E. Madey and J. T. Yates, in Rarefied Gas Dynamics, Proc. Sixth International Symposium, Cambridge, Mass., July 1968 (Academic Press, New York, in press).
12. This problem has been considered by L. K. Tower [Adv. Energy Conv. 3, 185 (1963)], but the results have not been tested by comparison with experimental data.
13. R. L. Palmer, H. Saltsburg, and J. N. Smith, in Fundamentals of Gas-Surface Interactions (Academic Press, New York, 1967), pp. 370-391.
14. R. E. Stickney, in Advances in Atomic and Molecular Physics, Vol. 3 (Academic Press, New York, 1967), pp. 143-204.
15. J. B. Anderson, R. P. Andres, and J. B. Fenn, in Advances in Atomic and Molecular Physics, Vol. 1 (Academic Press, New York, 1965), pp. 345-389.
16. E. H. Kennard, Kinetic Theory of Gases (McGraw-Hill Book Company, Inc., New York, 1938), pp. 61-64.
17. We shall use the term adsorption to denote temporary as well as permanent residence of an atom or molecule on a solid surface, with the stipulation that the residence time be sufficiently long relative to the characteristic time of lattice vibrations that the adsorbed species attain complete equilibrium both with the solid and with other adsorbed species before desorption occurs. We introduce the term equilibration probability because existing terms such as the sticking probability have special connotations.
18. The number of independent intensive thermodynamic properties necessary for specifying the equilibrium state depends on the number of independent components and phases of the system, and this dependence is described by the Gibbs phase rule. (For example, see K. Denbigh, The Principles of Chemical Equilibrium (Cambridge University Press, London, 1955), Chap. 5.)
19. A brief review of theoretical and experimental work relating to the equilibration probability has been presented by G. Ehrlich, in Annual Review of Physical Chemistry, Vol. 17, 1966, p. 295.

20. G. N. Lewis and M. Randall, Thermodynamics, 2d edition, revised by K. S. Pitzer and L. Brewer (McGraw-Hill Book Company, New York, 1961), Chaps. 15 and 33.

21. J. L. Margrave, The Characterization of High Temperature Vapors (John Wiley and Sons, Inc., New York, 1967).

22. For a recent review, see J. P. Hirth, Chap. 15 in J. L. Margrave, op. cit.

23. R. Fowler and E. A. Guggenheim, Statistical Thermodynamics (Cambridge University Press, London, 1956), see Eqs. (1106, 1) and (1111, 1).

24. W. B. Nottingham, "Thermionic Emission," in Handbuch der Physik, Vol. 21, S. Flügge (ed.) (Springer-Verlag, Berlin, 1956), pp. 1-175; also Technical Report 321, Research Laboratory of Electronics, M. I. T., Cambridge, Mass., December 10, 1956.

25. J. A. Fay, Molecular Thermodynamics (Addison-Wesley Publishing Company, Reading, Mass., 1965), p. 234.

26. The degeneracy of a free electron is $g_e = 2$, and Eq. 25 is based on the assumption that kT is small relative to the first electronic excitation potential.

27. For example, see J. N. Smith and W. L. Fite, J. Chem. Phys. 37, 898 (1962); J. D. McKinley, J. Chem. Phys. 40, 576 (1964); P. O. Schissel and O. C. Trulson, J. Chem. Phys. 43, 737 (1965).

28. G. E. Moore and F. C. Unterwald, J. Chem. Phys. 40, 2639 (1964).

29. B. McCarroll, J. Chem. Phys. 47, 5077 (1967).

30. R. A. Krakowski and D. R. Olander, J. Chem. Phys. (in press).

31. S. B. Nornes and E. E. Donaldson, J. Chem. Phys. 44, 2968 (1966).

32. T. W. Hickmott and G. Ehrlich, J. Phys. Chem. Solids 5, 47 (1958).

33. This expression for K_p is the square root of that derived in J. A. Fay, op. cit., pp. 229-233, because we are considering the reaction to be $\frac{1}{2} A_2 \rightleftharpoons A$ rather than $A_2 \rightleftharpoons 2A$.

34. J. E. Lennard-Jones, Trans. Faraday Soc. 28, 333 (1932).

35. For a discussion of activated adsorption, see D. O. Hayward and B. M. W. Trapnell, Chemisorption (Butterworths Science Publishers, London, 1964), Chap. 3, and G. C. Bond, Catalysis by Metals (Academic Press, New York, 1962), Chaps. 5 and 6.

36. P. Kisliuk, J. Phys. Chem. Solids 5, 78 (1958).

37. W. van Willigen, Phys. Letters 28A, 80 (1968).

38. Although it is expected that E_a is a periodic function related to the positions of the atoms of the solid surface, the variation in amplitude may be quite small because the molecule-solid potential involves more than nearest-neighbor interactions.

39. Equation 51 is based on the assumption that we may neglect the motion of the barrier caused by thermal fluctuations or by the gas-solid interaction itself. We would expect this assumption to be best in the case of a fast, light molecule such as H_2.

40. H. Saltsburgh and J. N. Smith: Unpublished results on the angular distribution of HD desorbing from a nickel surface serving as catalyst for the reaction $\frac{1}{2} H_2 + \frac{1}{2} D_2 \rightleftharpoons HD$. In the same study they have observed that the production of HD decreases with increasing angle of incidence of the D_2 molecular beam, thereby indicating that ζ'_{D_2} decreases as θ increases.

41. The equivalent of the quasi-equilibrium model for homogeneous reactions has proved to be an unacceptable approximation in certain cases, and it is inconsistent with rigorous kinetic analyses; see J. C. Keck and G. Carrier, J. Chem. Phys. 43, 2284 (1965).

42. The Rideal-Eley mechanism has been summarized by G. C. Bond, Catalysis by Metals (Academic Press, New York, 1962), p. 128.

43. R. H. Fowler, Statistical Mechanics (Cambridge University Press, London, 2d edition, 1936, reprinted 1966), p. 698.

44. R. C. Tolman, The Principles of Statistical Mechanics (Oxford University Press, London, 1938), pp. 161 and 521; also, Chap. 17 in R. H. Fowler, op. cit.

45. J. C. Keck, J. Chem. Phys. 29, 410 (1958).

46. Although the adsorbate coverage (the number of A atoms adsorbed per unit surface area) may be used in place of Σ' to describe the state of the adsorbate, Σ' is a more convenient parameter in the present treatment because it also appears in the conservation relation (Eq. B.7).

47. For a recent survey of gas-solid chemical reactions, see J. D. Fast, Interaction of Gases and Metals, Vol. 1 (Academic Press, New York, 1965).

48. P. Kofstad, High Temperature Oxidation of Metals (John Wiley and Sons, Inc., New York, 1966); O. Kubaschewski and B. E. Hopkins, Oxidation of Metals and Alloys (Butterworths Science Publishers, London, 1962).

49. D. Lieb and S. S. Kitrilakis, in Proc. Thermionic Conversion Specialist Conference (1966 IEEE Conference), pp. 348-354; F. Rufeh, D. Lieb, and F. Fraim, in Proc. Thermionic Conversion Specialist Conference (1967 IEEE Conference), pp. 25-28.

50. A. Y. Cho and H. Shelton, AIAA J. 2, 2135 (1964).

51. D. E. Rosner and H. D. Allendorf, J. Electrochem. Soc. 114, 305 (1967); G. A. Etemad, AIAA J. 4, 1543 (1966); B. W. Marshall, AIAA J. 4, 1899 (1966).

52. H. Shafer, Chemical Transport Reactions (Academic Press, New York, 1964), Sec. 3.2.

53. Ibid., see Sec. 3.4.

54. E. G. Zubler and F. A. Mosby, Illum. Eng. 54, 734 (1959); J. E. van Tijen, Phillips Tech. Rev. 23, 226 (1961-1962).

55. J. F. Waymouth, W. C. Gungle, J. M. Harris, and F. Koury, Illum. Eng. 60, 85 (1965).

56. D. L. Fehrs and R. E. Stickney, Surface Sci. 8, 267 (1967).

57. W. Engelmaier and R. E. Stickney, Surface Sci. 11, 370 (1968).

58. W. Greaves and R. E. Stickney, Surface Sci. 11, 395 (1968).

59. P. O. Schissel and O. C. Trulson, J. Chem. Phys. 43, 737 (1965).

60. J. B. Berkowitz-Mattuck, A. Buchler, J. L. Engelke, and S. N. Goldstein, J. Chem. Phys. 39, 2722 (1963).

61. W. C. Steele, Technical Report AFML-TR-65-343, Part II, Avco, Wilmington, Mass., January 1967.

62. Yu. G. Ptushinskii and B. A. Chuikov, Surface Sci. 6, 42 (1967); 7, 90 and 507 (1967).

63. B. McCarroll, J. Chem. Phys. 46, 863 (1967).

64. W. C. Steele (unpublished data).

65. R. F. Lever, Surface Sci. 9, 370 (1968), and in The Structure and Chemistry of Solid Surfaces, Proc. Fourth International Materials Symposium, Berkeley, California, 1968 (John Wiley and Sons, Inc., New York, in press).

66. B. McCarroll, J. Chem. Phys. 47, 5077 (1967).

67. J. N. Smith and W. L. Fite, in Rarefied Gas Dynamics, Proc. 3rd International Symposium, Paris, 1962, J. A. Laurmann (ed.) (Academic Press, New York, 1963), Vol. I, pp. 430-453.

68. J. D. McKinley, J. Chem. Phys. 40, 120 (1964).

69. J. D. McKinley, J. Chem. Phys. 41, 2814 (1964).

70. J. D. McKinley, J. Chem. Phys. 40, 576 (1964).

71. B. McCarroll, in The Structure and Chemistry of Solid Surfaces, Proc. Fourth International Materials Symposium, Berkeley, California, 1968 (John Wiley and Sons, Inc., New York, in press).

72. J. D. McKinley, J. Chem. Phys. 45, 1690 (1966).

73. E. H. Kennard, Kinetic Theory of Gases (McGraw-Hill Book Company, Inc., New York, 1938), p. 63.

74. According to the argument presented in Sec. I-D and I-F the properties (coverage, evaporation rates, etc.) of an equilibrated adsorbate phase are determined by specifying only the temperature, T, and the over-all adsorption rate, Σ_O. Therefore, the properties of an equilibrated adsorbate at a given temperature are the same for both equilibrium and nonequilibrium gas-phase conditions as long as the magnitude of Σ_O is the same in both cases.

75. See Chaps. 15 and 33 of G. N. Lewis and M. Randall, Thermodynamics, revised by K. S. Pitzer and L. Brewer (McGraw-Hill Book Company, Inc., New York, 1961).

76. JANAF Tables of Thermochemical Data, D. R. Stull (ed.) (Dow Chemical Co., Midland, Michigan, 1965, and Second Addendum, 1967).

77. D. O. Hayward and B. M. W. Trapnell, Chemisorption (Butterworths Science Publishers, London, 1964), Chap. 3.

78. If Z'_{O_2} is taken to be 7.5×10^{16} cm^{-2} sec^{-1}, then the value of ζ'_{O_2} computed from the experimental data on R_O for T > 2550°K (Fig. 7) would be greater than unity. We have therefore assumed that $Z'_{O_2} = 1.19 \times 10^{17}$ cm^{-2} sec^{-1}, as would be the case for $\zeta'_{O_2} = 1$ when T > 2900°K (Fig. 8). This change in Z'_{O_2} could be explained by postulating that the measured O_2 pressure is low by ~50%.

79. This estimate was obtained by using the present analysis (Eqs. 59, 63, and 64) to compute, by a trial-and-error method, the value of R_{O_2} that is consistent with the measured evaporation rates of the detectable species at that temperature.

80. The accuracy of the experimental evaporation rates is limited most seriously by the uncertainties of the ionization cross sections of oxide molecules, the mass dependence of the ion multiplier, and the measurements of temperature and pressure.

81. P. N. Walsh, J. M. Quets, and R. A. Graff, J. Chem. Phys. 46, 1144 (1967). References to other studies of the oxidation of tungsten are given in this paper.

82. G. De Maria, R. P. Burns, J. Drowart, and M. G. Inghram, J. Chem. Phys. 32, 1373 (1960).

83. R. P. Burns, G. De Maria, J. Drowart, and R. T. Grimley, J. Chem. Phys. 32, 1363 (1960).

84. D. R. Olander (unpublished results).

85. For example, dissociative adsorption of oxygen may produce species initially in highly excited vibrational states which may increase the probability that desorption will occur before the species have had time to equilibrate. This process is somewhat analogous to vibrational relaxation in gas-phase molecular recombination reactions.

86. For example, see J. P. Hirth, in The Characterization of High-Temperature Vapors, J. L. Margrave (ed.) (John Wiley and Sons, Inc., New York, 1967), pp. 453-472.

87. J. W. May and L. H. Germer, Surface Sci. 11, 443 (1968).

88. Yu. G. Ptushinskii and B. A. Chuikov, Surface Sci. 6, 42 (1967), and 7, 90 (1967).

89. See Eq. 63. Since the values of the equilibration probabilities (evaporation coefficients) are not known, we have assumed that all of them are unity.

90. A slight change in the T vs t relation causes a substantial change in the relative magnitudes of the computed curves in Figs. 21 and 22 because the instantaneous value of oxygen coverage at arbitrary time t and temperature T depends strongly upon the preceding temperature-time history.

91. J. H. Singleton, J. Chem. Phys. 47, 73 (1967); Ya. P. Zingerman and V. A. Ishchuk, Soviet Phys. – Solid State 9, 623 (1967), and 8, 2394 (1967); T. E. Madey and J. T. Yates, Surface Sci. 11, 327 (1968); N. J. Taylor, Surface Sci. 2, 544 (1964); J. Anderson and W. E. Danforth, J. Franklin Inst. 279, 160 (1965); L. H. Germer and J. W. May, Surface Sci. 4, 452 (1966); P. J. Estrup and J. Anderson, in Report on Twenty-seventh Annual Conference on Physical Electronics, M. I. T., Cambridge, Mass., 1967, pp. 47-53.

92. For a discussion of this expression for R_O, see D. O. Hayward and B. M. W. Trapnell, Chemisorption (Butterworths Science Publishers, London, 1964), Chap. 4.

93. B. McCarroll, Surface Sci. 7, 499 (1967).

94. Yu. G. Ptushinskii and B. A. Chuikov, Surface Sci. 7, 507 (1967).

95. Equation 70 may be used to show that

$$K_{W_xO_y}/K_O^y = \exp\{-[(\Delta H^\circ_{W_xO_y} - y\,\Delta H^\circ_O) - T(\Delta S^\circ_{W_xO_y} - y\,\Delta S^\circ_O)]/RT\}.$$

With the values of ΔH° and ΔS° listed in the JANAF Tables of Thermochemical Data, D. R. Stull (ed.), (Dow Chemical Co., Midland, Mich., 1965 and Second Addendum, 1967), it is possible to prove that $K_{W_xO_y}/K_O^y$ decreases with increasing temperature for WO_2, WO_3, W_2O_6, and W_3O_9.

96. Yu. G. Ptushinskii and B. A. Chuikov, Soviet Phys. – Solid State 10, 565 (1968).

97. R. T. Grimley, in The Characterization of High-Temperature Vapors, J. L. Margrave (ed.) (John Wiley and Sons, Inc., New York, 1967), pp. 222-225.

98. J. W. Otvos and D. P. Stevenson, J. Am. Chem. Soc. 78, 546 (1956).

99. As an illustration of this method of calibration, see Schissel and Trulson.[59]

100. J. A. Becker, E. J. Becker, and R. G. Brandes, J. Appl. Phys. 32, 411 (1961); V. S. Ageikin and Yu. G. Ptushinskii, Ukrain. Fiz. Zhurn. 12, 1483 (1967).

101. For example, the relative magnitudes of the O, WO_2, and WO_3 peaks in the flash desorption curves measured by Ptushinskii and Chuikov[88] and by McCarroll[29] agree within a fraction of two.

JOINT SERVICES ELECTRONICS PROGRAM
REPORTS DISTRIBUTION LIST

Department of Defense

Dr. A. A. Dougal
Asst Director (Research)
Ofc of Defense Res & Eng
Department of Defense
Washington, D. C. 20301

Office of Deputy Director
(Research and Information, Rm 3D1037)
Department of Defense
The Pentagon
Washington, D. C. 20301

Director
Advanced Research Projects Agency
Department of Defense
Washington, D. C. 20301

Director for Materials Sciences
Advanced Research Projects Agency
Department of Defense
Washington, D. C. 20301

Headquarters
Defense Communications Agency (340)
Washington, D. C. 20305

Defense Documentation Center
Attn: DDC-TCA
Cameron Station
Alexandria, Virginia 22314

Director
National Security Agency
Attn: TDL
Fort George G. Meade, Maryland 20755

Weapons Systems Evaluation Group
Attn: Colonel Blaine O. Vogt
400 Army-Navy Drive
Arlington, Virginia 22202

Central Intelligence Agency
Attn: OCR/DD Publications
Washington, D. C. 20505

Department of the Air Force

Hq USAF (AFRDDD)
The Pentagon
Washington, D. C. 20330

Hq USAF (AFRDDG)
The Pentagon
Washington, D. C. 20330

Hq USAF (AFRDSD)
The Pentagon
Washington, D. C. 20330

Colonel E. P. Gaines, Jr.
ACDA/FO
1901 Pennsylvania Avenue N. W.
Washington, D. C. 20451

Lt Col R. B. Kalisch (SREE)
Chief, Electronics Division
Directorate of Engineering Sciences
Air Force Office of Scientific Research
Arlington, Virginia 22209

Dr. I. R. Mirman
AFSC (SCT)
Andrews Air Force Base, Maryland 20331

AFSC (SCTSE)
Andrews Air Force Base, Maryland 20331

Mr. Morton M. Pavane, Chief
AFSC Scientific and Technical Liaison
Office
26 Federal Plaza, Suite 1313
New York, New York 10007

Rome Air Development Center
Attn: Documents Library (EMTLD)
Griffiss Air Force Base, New York 13440

Mr. H. E. Webb (EMIIS)
Rome Air Development Center
Griffiss Air Force Base, New York 13440

Dr. L. M. Hollingsworth
AFCRL (CRN)
L. G. Hanscom Field
Bedford, Massachusetts 01730

AFCRL (CRMPLR), Stop 29
AFCRL Research Library
L. G. Hanscom Field
Bedford, Massachusetts 01730

Hq ESD (ESTI)
L. G. Hanscom Field
Bedford, Massachusetts 01730

Professor J. J. D'Azzo
Dept of Electrical Engineering
Air Force Institute of Technology,
Wright-Patterson Air Force Base,
Ohio 45433

JOINT SERVICES REPORTS DISTRIBUTION LIST (continued)

Dr. H. V. Noble (CAVT)
Air Force Avionics Laboratory
Wright-Patterson Air Force Base,
Ohio 45433

Director
Air Force Avionics Laboratory
Wright-Patterson Air Force Base,
Ohio 45433

AFAL (AVTA/R. D. Larson)
Wright-Patterson Air Force Base,
Ohio 45433

Director of Faculty Research
Department of the Air Force
U.S. Air Force Academy
Colorado Springs, Colorado 80840

Academy Library (DFSLB)
USAF Academy
Colorado Springs, Colorado 80840

Director
Aerospace Mechanics Division
Frank J. Seiler Research Laboratory (OAR)
USAF Academy
Colorado Springs, Colorado 80840

Director, USAF PROJECT RAND
Via: Air Force Liaison Office
The RAND Corporation
Attn: Library D
1700 Main Street
Santa Monica, California 90406

Hq SAMSO (SMTTA/Lt Nelson)
Air Force Unit Post Office
Los Angeles, California 90045

Det 6, Hq OAR
Air Force Unit Post Office
Los Angeles, California 90045

AUL3T-9663
Maxwell Air Force Base, Alabama 36112

AFETR Technical Library
(ETV, MU-135)
Patrick Air Force Base, Florida 32925

ADTC (ADBPS-12)
Eglin Air Force Base, Florida 32542

Mr. B. R. Locke
Technical Adviser, Requirements
USAF Security Service
Kelly Air Force Base, Texas 78241

Hq AMD (AMR)
Brooks Air Force Base, Texas 78235

USAFSAM (SMKOR)
Brooks Air Force Base, Texas 78235

Commanding General
Attn: STEWS-RE-L, Technical Library
White Sands Missile Range,
New Mexico 88002

Hq AEDC (AETS)
Attn: Library/Documents
Arnold Air Force Station, Tennessee 37389

European Office of Aerospace Research
APO New York 09667

Department of the Army

Physical & Engineering Sciences Division
U.S. Army Research Office
3045 Columbia Pike
Arlington, Virginia 22204

Commanding General
U.S. Army Security Agency
Attn: IARD-T
Arlington Hall Station
Arlington, Virginia 22212

Commanding General
U.S. Army Materiel Command
Attn: AMCRD-TP
Washington, D. C. 20315

Commanding Officer
Harry Diamond Laboratories
Attn: Dr. Berthold Altman (AMXDO-TI)
Connecticut Avenue and
Van Ness Street N. W.
Washington, D. C. 20438

Director
Walter Reed Army Institute of Research
Walter Reed Army Medical Center
Washington, D. C. 20012

Commanding Officer (AMXRD-BAT)
U.S. Army Ballistics Research Laboratory
Aberdeen Proving Ground
Aberdeen, Maryland 21005

Technical Director
U.S. Army Limited War Laboratory
Aberdeen Proving Ground
Aberdeen, Maryland 21005

Commanding Officer
Human Engineering Laboratories
Aberdeen Proving Ground
Aberdeen, Maryland 21005

U.S. Army Munitions Command
Attn: Science & Technology Information Branch, Bldg 59
Picatinny Arsenal, SMUPA-VA6
Dover, New Jersey 07801

U.S. Army Mobility Equipment Research and Development Center
Attn: Technical Document Center, Bldg 315
Fort Belvoir, Virginia 22060

Director
U.S. Army Engineer Geodesy, Intelligence & Mapping
Research and Development Agency
Fort Belvoir, Virginia 22060

Dr. Herman Robl
Deputy Chief Scientist
U.S. Army Research Office (Durham)
Box CM, Duke Station
Durham, North Carolina 27706

Richard O. Ulsh (CRDARD-IPO)
U.S. Army Research Office (Durham)
Box CM, Duke Station
Durham, North Carolina 27706

Technical Director (SMUFA-A2000-107-1)
Frankford Arsenal
Philadelphia, Pennsylvania 19137

Redstone Scientific Information Center
Attn: Chief Document Section
U.S. Army Missile Command
Redstone Arsenal, Alabama 35809

Commanding General
U.S. Army Missile Command
Attn: AMSMI-REX
Redstone Arsenal, Alabama 35809

Commanding General
U.S. Army Strategic Communications Command
Attn: SCC-CG-SAE
Fort Huachuca, Arizona 85613

Commanding Officer
Army Materials and Mechanics Research Center
Attn: Dr. H. Priest
Watertown Arsenal
Watertown, Massachusetts 02172

Commandant
U.S. Army Air Defense School
Attn: Missile Science Division, C&S Dept,
P. O. Box 9390
Fort Bliss, Texas 79916

Commandant
U.S. Army Command and General Staff College
Attn: Acquisitions, Lib Div
Fort Leavenworth, Kansas 66027

Commanding Officer
U.S. Army Electronics R&D Activity
White Sands Missile Range,
New Mexico 88002

Mr. Norman J. Field, AMSEL-RD-S
Chief, Office of Science & Technology
Research and Development Directorate
U.S. Army Electronics Command
Fort Monmouth, New Jersey 07703

Mr. Robert O. Parker, AMSEL-RD-S
Executive Secretary, JSTAC
U. S. Army Electronics Command
Fort Monmouth, New Jersey 07703

Commanding General
U.S. Army Electronics Command
Fort Monmouth, New Jersey 07703
Attn: AMSEL-SC
RD-GF
RD-MT
XL-D
XL-E
XL-C
XL-S (Dr. R. Buser)
HL-CT-DD
HL-CT-R
HL-CT-L (Dr. W.S.McAfee)
HL-CT-O
HL-CT-I
HL-CT-A
NL-D
NL-A
NL-P
NL-P-2 (Mr. D. Haratz)
NL-R (Mr. R. Kulinyi)
NL-S
KL-D
KL-E
KL-S (Dr. H. Jacobs)
KL-SM (Drs. Schiel/Hieslmair)
KL-T
VL-D
VL-F (Mr. R.J. Niemela)
WL-D

Dr. A. D. Schnitzler, AMSEL-HL-NVII
Night Vision Laboratory, USAECOM
Fort Belvoir, Virginia 22060

Dr. G. M. Janney, AMSEL-HL-NVOR
Night Vision Laboratory, USAECOM
Fort Belvoir, Virginia 22060

Atmospheric Sciences Office
Atmospheric Sciences Laboratory
White Sands Missile Range,
New Mexico 88002

Missile Electronic Warfare Technical
Area, (AMSEL-WT-MT)
White Sands Missile Range,
New Mexico 88002

Deputy for Research and Engineering
(AMSWE-DRE)
U.S. Army Weapons Command
Rock Island Arsenal
Rock Island, Illinois 61201

Project Manager
Common Positioning & Navigation Systems
Attn: Harold H. Bahr (AMCPM-NS-TM),
Bldg 439
U.S. Army Electronics Command
Fort Monmouth, New Jersey 07703

Director
U.S. Army Advanced Materiel
Concepts Agency
Washington, D. C. 20315

Department of the Navy

Director, Electronic Programs
Attn: Code 427
Department of the Navy
Washington, D. C. 20360

Commander
U.S. Naval Security Group Command
Attn: G43
3801 Nebraska Avenue
Washington, D. C. 20390

Director
Naval Research Laboratory
Washington, D. C. 20390
Attn: Code 2027
Dr. W. C. Hall, Code 7000
Dr. A. Brodzinsky, Supt. Elec. Div.

Dr. G. M. R. Winkler
Director, Time Service Division
U.S. Naval Observatory
Washington, D. C. 20390

Naval Air Systems Command
AIR 03
Washington, D. C. 20360

Naval Ship Systems Command
Ship 031
Washington, D. C. 20360

Naval Ship Systems Command
Ship 035
Washington, D. C. 20360

U. S. Naval Weapons Laboratory
Dahlgren, Virginia 22448

Naval Electronic Systems Command
ELEX 03, Room 2046 Munitions Building
Department of the Navy
Washington, D. C. 20360

Head, Technical Services Division
Naval Investigative Service Headquarters
4420 North Fairfax Drive
Arlington, Virginia 22203

Commander
U.S. Naval Ordnance Laboratory
Attn: Librarian
White Oak, Maryland 21502

Commanding Officer
Office of Naval Research Branch Office
Box 39 FPO
New York, New York 09510

Commanding Officer
Office of Naval Research Branch Office
219 South Dearborn Street
Chicago, Illinois 60604

Commanding Officer
Office of Naval Research Branch Office
495 Summer Street
Boston, Massachusetts 02210

Commander (ADL)
Naval Air Development Center
Johnsville, Warminster,
Pennsylvania 18974

Commanding Officer
Naval Training Device Center
Orlando, Florida 32813

Commander (Code 753)
Naval Weapons Center
Attn: Technical Library
China Lake, California 93555

Commanding Officer
Naval Weapons Center
Corona Laboratories
Attn: Library
Corona, California 91720

Commander
U.S. Naval Missile Center
Point Mugu, California 93041

W. A. Eberspacher, Associate Head
Systems Integration Division
Code 5340A, Box 15
U.S. Naval Missile Center
Point Mugu, California 93041

Commander
Naval Electronics Laboratory Center
Attn: Library
San Diego, California 92152

Deputy Director and Chief Scientist
Office of Naval Research Branch Office
1030 East Green Street
Pasadena, California 91101

Library (Code 2124)
Technical Report Section
Naval Postgraduate School
Monterey, California 93940

Glen A. Myers (Code 52 Mv)
Assoc. Prof. of Electrical Engineering
Naval Postgraduate School
Monterey, California 93940

Commanding Officer and Director
U.S. Naval Underwater Sound Laboratory
Fort Trumbull
New London, Connecticut 06840

Commanding Officer
Naval Avionics Facility
Indianapolis, Indiana 46241

Other Government Agencies

Dr. H. Harrison, Code RRE
Chief, Electrophysics Branch
National Aeronautics and
Space Administration
Washington, D. C. 20546

NASA Lewis Research Center
Attn: Library
21000 Brookpark Road
Cleveland, Ohio 44135

Los Alamos Scientific Laboratory
Attn: Reports Library
P. O. Box 1663
Los Alamos, New Mexico 87544

Federal Aviation Administration
Attn: Admin Stds Div (MS-110)
800 Independence Avenue S. W.
Washington, D. C. 20590

Mr. M. Zane Thornton, Chief
Network Engineering, Communications
and Operations Branch
Lister Hill National Center for
Biomedical Communications
8600 Rockville Pike
Bethesda, Maryland 20014

U. S. Post Office Department
Library - Room 6012
12th & Pennsylvania Avenue, N. W.
Washington, D. C. 20260

Non-Government Agencies

Director
Research Laboratory of Electronics
Massachusetts Institute of Technology
Cambridge, Massachusetts 02139

Mr. Jerome Fox, Research Coordinator
Polytechnic Institute of Brooklyn
333 Jay Street
Brooklyn, New York 11201

Director
Columbia Radiation Laboratory
Columbia University
538 West 120th Street
New York, New York 10027

Director
Coordinated Science Laboratory
University of Illinois
Urbana, Illinois 61801

Director
Stanford Electronics Laboratories
Stanford University
Stanford, California 94305

Director
Microwave Physics Laboratory
Stanford University
Stanford, California 94305

Director
Electronics Research Laboratory
University of California
Berkeley, California 94720

Director
Electronic Sciences Laboratory
University of Southern California
Los Angeles, California 90007

Director
Electronics Research Center
The University of Texas at Austin
Austin, Texas 78712

Division of Engineering and
Applied Physics
Harvard University
Cambridge, Massachusetts 02138

Dr. G. J. Murphy
The Technological Institute
Northwestern University
Evanston, Illinois 60201

Dr. John C. Hancock, Head
School of Electrical Engineering
Purdue University
Lafayette, Indiana 47907

Department of Electrical Engineering
Texas Technological College
Lubbock, Texas 79409

Aerospace Corporation
P. O. Box 95085
Los Angeles, California 90045
Attn: Library Acquisition Group

Prof. Nicholas George
California Institute of Technology
Pasadena, California 91109

Aeronautics Library
Graduate Aeronautical Laboratories
California Institute of Technology
1201 E. California Blvd.
Pasadena, California 91109

The Johns Hopkins University
Applied Physics Laboratory
Attn: Document Librarian
8621 Georgia Avenue
Silver Spring, Maryland 20910

Hunt Library
Carnegie-Mellon University
Schenley Park
Pittsburgh, Pennsylvania 15213

Dr. Leo Young
Stanford Research Institute
Menlo Park, California 94025

School of Engineering Sciences
Arizona State University
Tempe, Arizona 85281

Engineering and Mathematical
Sciences Library
University of California at Los Angeles
405 Hilgard Avenue
Los Angeles, California 90024

The Library
Government Publications Section
University of California
Santa Barbara, California 93106

Carnegie-Mellon University
Electrical Engineering Department
Pittsburgh, Pennsylvania 15213

Prof. Joseph E. Rowe
Chairman, Dept of Electrical Engineering
The University of Michigan
Ann Arbor, Michigan 48104

New York University
College of Engineering
New York, New York 10019

Syracuse University
Department of Electrical Engineering
Syracuse, New York 13210

Yale University
Engineering Department
New Haven, Connecticut 06520

Airborne Instruments Laboratory
Deerpark, New York 11729

Raytheon Company
Attn: Librarian
Bedford, Massachusetts 01730

JOINT SERVICES REPORTS DISTRIBUTION LIST (continued)

Raytheon Company
Research Division Library
28 Seyon Street
Waltham, Massachusetts 02154

Dr. Sheldon J. Welles
Electronic Properties Information Center
Mail Station E-175
Hughes Aircraft Company
Culver City, California 90230

Dr. Robert E. Fontana
Systems Research Laboratories Inc.
7001 Indian Ripple Road
Dayton, Ohio 45440

Nuclear Instrumentation Group
Bldg 29, Room 101
Lawrence Radiation Laboratory
University of California
Berkeley, California 94720

Sylvania Electronic Systems
Applied Research Laboratory
Attn: Documents Librarian
40 Sylvan Road
Waltham, Massachusetts 02154

Hollander Associates
P. O. Box 2276
Fullerton, California 92633

Illinois Institute of Technology
Department of Electrical Engineering
Chicago, Illinois 60616

The University of Arizona
Department of Electrical Engineering
Tucson, Arizona 85721

Utah State University
Department of Electrical Engineering
Logan, Utah 84321

Case Western Reserve University
Engineering Division
University Circle
Cleveland, Ohio 44106

Lincoln Laboratory
Massachusetts Institute of Technology
Lexington, Massachusetts 02173

The University of Iowa
The University Libraries
Iowa City, Iowa 52240

Lenkurt Electric Co., Inc.
1105 County Road
San Carlos, California 94070
Attn: Mr. E. K. Peterson

Philco Ford Corporation
Communications & Electronics Division
Union Meeting and Jolly Roads
Blue Bell, Pennsylvania 19422

Union Carbide Corporation
Electronic Division
P. O. Box 1209
Mountain View, California 94041

Department of Electrical Engineering
Rice University
Houston, Texas 77001

Research Laboratories for the
Engineering Sciences
School of Engineering and Applied Science
University of Virginia
Charlottesville, Virginia 22903

Department of Electrical Engineering
College of Engineering and Technology
Ohio University
Athens, Ohio 45701

Project MAC
Document Room
Massachusetts Institute of Technology
545 Technology Square
Cambridge, Massachusetts 02139

Department of Electrical Engineering
Lehigh University
Bethlehem, Pennsylvania 18015

UNCLASSIFIED
Security Classification

DOCUMENT CONTROL DATA - R & D

(Security classification of title, body of abstract and indexing annotation must be entered when the overall report is classified)

1. ORIGINATING ACTIVITY *(Corporate author)*
Research Laboratory of Electronics
Massachusetts Institute of Technology
Cambridge, Massachusetts 02139

2a. REPORT SECURITY CLASSIFICATION
Unclassified

2b. GROUP
None

3. REPORT TITLE
Thermodynamics and Kinetics of Heterogeneous Reactions

4. DESCRIPTIVE NOTES *(Type of report and inclusive dates)*
Technical Report

5. AUTHOR(S) *(First name, middle initial, last name)*
J. Clair Batty
Robert E. Stickney

6. REPORT DATE
June 2, 1969

7a. TOTAL NO. OF PAGES
80

7b. NO. OF REFS
101

8a. CONTRACT OR GRANT NO.
Da 28-043-AMC-02536(E)

b. PROJECT NO.
200-14501-B31F

c. NASA Grant NGR 22-009-091

d. M. I. T. Cabot Solar Energy Fund

9a. ORIGINATOR'S REPORT NUMBER(S)
Technical Report 473

9b. OTHER REPORT NO(S) *(Any other numbers that may be assigned this report)*

10. DISTRIBUTION STATEMENT
This document has been approved for public release and sale; its distribution is unlimited.

11. SUPPLEMENTARY NOTES

12. SPONSORING MILITARY ACTIVITY
Joint Services Electronics Program
Through U. S. Army Electronics Command

13. ABSTRACT

A generalized treatment of heterogeneous chemical reactions is developed and applied to several sublimation, catalytic, and oxidation processes. The approach is essentially a systematic reformulation of the quasi-equilibrium analyses of Langmuir, Richardson, and others, and it is generalized to apply also to conditions encountered in molecular-beam studies of gas-solid interactions. An advantage of the quasi-equilibrium approach is that it minimizes the use of kinetics to the degree that rate expressions are obtained without assuming detailed kinetic models of the processes.

In Part I, we consider simple sublimation processes (vaporization, thermionic emission, and self-surface ionization) and catalytic reactions (surface ionization and molecular dissociation). The reaction of gaseous oxygen with solid tungsten, molybdenum, and graphite is treated in Part II for steady-state conditions, and this treatment is extended in Part III to the transient case of flash desorption of oxides from a tungsten surface. The theoretical results are compared with existing experimental data, and the agreement is surprisingly good in view of the simplicity of the approach.

DD FORM 1 NOV 65 1473 (PAGE 1)

UNCLASSIFIED
Security Classification

14. KEY WORDS	LINK A		LINK B		LINK C	
	ROLE	WT	ROLE	WT	ROLE	WT
ablation						
equilibrium probability						
gas-solid interactions						
gas-solid interface						
heterogeneous chemical reactions, generalized treatment of						
high-temperature graphite, oxidation of						
high-temperature molybdenum, oxidation of						
high-temperature tungsten, oxidation of						
mass-spectrometric studies						
molecular-beam studies						
sticking probability						
sublimation of solids						
surface catalysis						
surface ionization						
thermionic emission						